

Objective-Free Local Learning and Emergent Language Structure in Thinking Machines

P. Myles Eugenio

pamyeu@iu.edu

Department of Physics, Indiana University
Bloomington, Indiana 47405, USA

ABSTRACT

We introduce a neuro-symbolic framework for generative language modeling, based on local event-drive emergent learning. The framework is centered around hierarchical Hopfield memory chains, which act as a compositional short-term memory & dynamic tokenizer (*def.* retokenizer). Rather than relying on predefined tokens or supervised training, the model builds structure from scratch, learning to retokenize symbol sequences into multi-scale, compositional representations. It does this by hierarchically constructing projection tensors, which glue together symbol sequences into *multi-scale* tokens. This imbues the model with an inherent redundancy (i.e. an emergent gauge structure), and allows the model to compress local feature co-activations into long-range dependencies.

Curiously, we find that the retokenizer can filter natural language patterns from noise, generating synthetic languages with coherent internal morphology – quantifiably the same as human language. Language is learned in a local (Hebbian) fashion, where model constraints dictate allowed emergent structure, and new information is retained in alignment with this structure.

The lack of global objective allows for a type of plasticity not seen in other language models, including allowing it to generalize beyond its initial inference class (and can do so without explicit data). We show that briefly exposing a single new neuron to the retokenizer during inference, binds the distributed multi-scale token features into a symbolic embedding neuron. These embedding neurons behave as an emergent long-term memory, and introduces a key-value memory mechanism that enables compositional inference and generalization.

This architecture provides a methodological foundation for studying how symbolic structure can emerge from local neural learning. It offers a new pathway for building scalable, interpretable neuro-symbolic systems – where tokens, grammar, and reasoning arise as compressed memory traces within a fully unsupervised Hopfield hierarchy. This approach advances the development of scalable, neuromorphic architectures for generative language models.

KEYWORDS

Exotic AI, Hebbian, Hopfield Networks, Physics-inspired Neural Nets, Interpretable Models, Hierarchical Compression, Language Emergence, Neuro-symbolic, Neuromorphic

1 INTRODUCTION

Objective-free local learning is the paradigm by which much of the observed structure and organization in the universe arises. In this setting, learning is governed solely by local rules—no global objective functions, no central coordination. Such systems evolve asynchronously, with higher-order and longer-range correlations

emerging as incidental consequences of local interactions unfolding over time.

This paradigm includes many natural and artificial systems: human cognition, biochemical self-organization, and even simple cellular automata such as Conway’s Game of Life. Crucially, learning can emerge from random initial conditions without prestructured input. This implies that structure can be learned in a truly *data-free* regime, where the learning system constructs its own vocabulary and concepts directly from noise.

In a companion paper [14], we derived an effective human language model based on this principle: a *hierarchical-chain Hopfield network* trained via local Hebbian updates. There, we showed how unsupervised hierarchical feature construction can filter linguistic patterns from noise, giving rise to morphologically coherent vocabularies without supervision or data.

Here, we lay out the broader methodological framework inspired by that model. We describe how local learning events can organize into a recursive projection hierarchy, how memory emerges through replay, and how the resulting system supports key capacities of generative language modeling—tokenization, compositional structure, fast autoregressive inference, and compression—without requiring a global objective, backpropagation, nor explicit data.

This framework also bridges two traditionally distinct approaches to language modeling: correlation-based neural systems [28, 30, 31, 48, 54, 63] and symbolic compositional reasoning [10, 12, 13, 35, 36, 65]. At the lower levels, the model constructs a directed acyclic graph (DAG) of valid n -gram combinations, gradually building a recursively compositional vocabulary through a process we call *retokenization*. Each layer of the hierarchy learns local statistical correlations—akin to identifying relevant interactions in a renormalization group flow [56, 57, 67]—and projects them into higher-level tokens. In this way, the system builds structured representations across scales, where short-range associations give rise to long-range compositional units.

This sub-symbolic mechanism allows the model to infer token boundaries without explicit markers (e.g. space or stop tokens), defining a notion of string *acceptance* grounded in learned statistical compatibility. The projector maps encode a hierarchy of memory that approximates automaton-like behavior¹: a sequence is tokenized only if it conforms to the model’s internal structure, and next-token predictions follow trajectories constrained by these

¹Formally, regular languages are recognized by finite-state automata that lack explicit memory for counting or nesting [27]. The early stages of our model resemble finite-state structures through local n -gram interactions. However, continual learning causes the model to generalize beyond its initial inference class, and may implicitly support more complex behaviors beyond finite-state expressivity [25, 45–47, 50, 51, 64]. A rigorous classification of the exact formal grammar class supported by this model remains a promising direction for future work.

memory-induced transitions. Thus, inference behaves like a grammar operating over a learned token space, where the distinction between automaton, grammar, & memory storage/retrieval is blurred. Rather than explicitly storing rules, the system implements them implicitly through its architecture, enabling the replay and recombination of stored sequences without relying on explicit symbolic guidance.

Critically, the model acquires long-term memory not through fixed architecture but through a dynamic inference-driven learning process we call *replay*. This mechanism enables the system to regenerate and reorganize previously learned structures, binding them into higher-level embedding neurons. These embeddings act as a sparse key-value memory [4, 18, 62], supporting pattern completion and selective recall. Once replay is used to compress and store learned patterns, the lower-layer short-term memory can be forgotten or reused — a form of memory indirection that enables continual learning and concept recombination. In this way, the model achieves Turing-like memory dynamics [23, 24]: hierarchical information can persist even as local memory is overwritten, supporting compositional generalization and long-range inference.

A central strength of this framework lies in its interpretability. Each step in the learning process — from Hebbian updates to hierarchical token composition — is locally defined and analytically tractable. The structure and evolution of the model can be explicitly visualized through small toy examples, enabling direct inspection of how words are learned, compressed, and replayed. Unlike black-box models, the memory tensors and projector maps in each layer can be examined and manipulated, allowing one to trace the flow of information across layers and interpret model decisions in terms of compositional features. This makes the framework not only an effective generative model but also a platform for theoretical analysis and conceptual clarity — a rare intersection of symbolic transparency and neural dynamics.

Because of this, we have organized the first half of the paper (Sec 2-6) as both the model introduction & practical tutorial. Sec 2-3 discuss short-term memory (STM). Sec 4-5 discusses long-term memory (LTM) & their emergent key-value mechanisms. In Sec 7, we demonstrate how compositional STM can be creative. We touch on the deeper relationship between inductive biases and natural language structure in Sec 7.1. We end with an extended discussion.

2 MODEL SUMMARY: LOCAL EVENTS AND HIERARCHICAL RETOKENIZATION

2.1 Local Learning Events

The foundational object of our framework is a localized *event*, defined as a pair

$$\mathcal{E}^{(n)} = (\tilde{v}_{\mu_{n-1}}^{(n-1)}, v_k),$$

where v_k is the free token to be predicted, and $\tilde{v}_{\mu_{n-1}}^{(n-1)}$ is the learned projection of the $n-1$ trailing context tokens. Each such event represents a local time-step in the dynamics of the model, and triggers a Hebbian memory update:

$$g_{\mu_{n-1},k}^{(n)} \leftarrow g_{\mu_{n-1},k}^{(n)} + \tilde{v}_{\mu_{n-1}}^{(n-1)} v_k. \quad (1)$$

This update defines a *short-term memory synapse*, storing pairwise correlations between projected context features and the next token.

Learning is entirely local and unsupervised: there is no global loss function, and no backpropagation.

2.2 Hierarchical Retokenization

To organize these events across scales, the model constructs a recursive sequence of projection maps P_n that define higher-order features. Each projection promotes a pair $(\tilde{v}^{(n-1)}, v)$ to a new token $\tilde{v}^{(n)}$, if it satisfies the condition:

$$\tilde{v}_{\mu_n}^{(n)} = \sum_{\mu_{n-1},k} P_n^{\mu_n, \mu_{n-1}, k} \tilde{v}_{\mu_{n-1}}^{(n-1)} v_k, \quad P_n^{\mu_n, \mu_{n-1}, k} \in \{0, 1\}. \quad (2)$$

These retokenized features form the model’s internal vocabulary. Importantly, the projection maps are constrained by a *smoothness condition*: a new n -gram token is allowed only if all its subcomponents are already valid $(n-1)$ -grams. This ensures that every token in the hierarchy is recursively decomposable — i.e. retokenizable.

2.3 Hierarchical Energy and Inference

The total model energy over all layers is:

$$H = \sum_{n \geq 2} \sum_{\mu_{n-1},k} g_{\mu_{n-1},k}^{(n)} \tilde{v}_{\mu_{n-1}}^{(n-1)} v_k. \quad (3)$$

Inference corresponds to computing the energy gradient with respect to the next token:

$$\frac{\partial H}{\partial v_k} = \sum_{n \geq 2} \sum_{\mu_{n-1}} g_{\mu_{n-1},k}^{(n)} \tilde{v}_{\mu_{n-1}}^{(n-1)}, \quad (4)$$

with update rule $v_k \leftarrow f_k(\frac{\partial H}{\partial v_k})$, where f is a bounded function acting on every element of v_k . This quantity defines a fast autoregressive prediction mechanism: each token is generated by summing over its correlations with retokenized contexts across multiple scales. The value of the next token is sampled from a probability distribution, e.g. $\rho_k(v_k) = e^{v_k} / \sum_j e^{v_j}$. Note, the model can be biased to favor longer-range dependencies by rescaling weights of deeper layers: $g^{(n)} \rightarrow \beta^n g^{(n)}$ with $\beta > 1$.

3 RETOKENIZATION AND EMERGENT n -POINT STRUCTURE

Although each layer of the model stores only local 2-point correlations between a projected context token and a predicted token,

$$H_n = \sum_{\mu_{n-1},k} g_{\mu_{n-1},k}^{(n)} \tilde{v}_{\mu_{n-1}}^{(n-1)} v_k,$$

the recursive definition of projected tokens induces an implicit n -point interaction. Each projection is defined via Eqn 2 and applying this recursively from the basis layer ($n = 1$) yields:

$$\tilde{v}_{\mu_{n-1}}^{(n-1)} = \sum_{j_1, \dots, j_{n-1}} (P_{n-1} \cdots P_3 P_2)_{j_1 \cdots j_{n-1}}^{\mu_{n-1}} v_{j_1} v_{j_2} \cdots v_{j_{n-1}}, \quad (5)$$

$$\Rightarrow H_n = \sum_{j_1, \dots, j_n} g_{j_1 \cdots j_n}^{(n)} v_{j_1} \cdots v_{j_n}, \quad (6)$$

where

$$g_{j_1 \cdots j_n}^{(n)} = \sum_{\mu_{n-1}} g_{\mu_{n-1}, j_n}^{(n)} \cdot (P_{n-1} \cdots P_2)_{j_1 \cdots j_{n-1}}^{\mu_{n-1}}.$$

Thus, a learned 2-point memory update at level n becomes an effective n -point interaction through hierarchical retokenization.

This allows the model to encode long-range dependencies in a compressed form using only local unsupervised learning events.

3.1 Retokenization Symmetries and Gauge Equivalence

The same tensor $\tilde{v}^{(n)}$ can be expressed with either left- or right-tokenized orderings of its internal structure. These forms are related via recursive retokenization of the projection tensors. Given a right-tokenized projector $P_n^{\mu_n, \mu_{n-1}, k}$, we define the corresponding left-tokenized form recursively as:

$$P_{L,n}^{\mu_n, j_1, \mu_{n-1}} = \sum_{k, \mu_{n-2}} \left(\sum_{\mu_{n-1}} P_n^{\mu_n, \mu_{n-1}, k} \cdot P_{L, n-1}^{\mu_{n-1}, j_1, \mu_{n-2}} \right) \cdot P_{n-1}^{\mu_{n-1}, \mu_{n-2}, k}, \quad (7)$$

with base case $P_{L,2}^{\mu_2, j_1, j_2} := P_2^{\mu_2, j_1, j_2}$. These transformations preserve the *smooth gauge structure* of the model, and maps us between different representations of the same smooth tensor, which are distinguished by the order & number of indices. (E.g $g_{\mu_n}^{(n)}$, $g_{\mu_{n-1}, k}^{(n)}$, & $g_{k, \mu_{n-1}}^{(n)}$ are different representations of $g^{(n)}$.) Where reordering is done via retokenization and *not* transposition ($g_{\mu_{n-1}, k}^{(n)} \neq g_{k, \mu_{n-1}}^{(n)T}$ in general). In practice, this means:

$$\sum_{\mu_{n-1}, k} P_n^{\mu_n, \mu_{n-1}, k} \tilde{v}_{\mu_{n-1}}^{(n-1)} v_k = \sum_{k, \mu_{n-1}} P_{L,n}^{\mu_n, k, \mu_{n-1}} v_k \tilde{v}_{\mu_{n-1}}^{(n-1)}.$$

This formalism ensures that all token representations and learning updates remain strictly local and compositional, while implicitly capturing longer correlations.

We may understand this redundancy of the hierarchical feature-set as manifesting an emergent associativity, such that the tensor product $v_c v_a v_t$ can be recast as $\tilde{v}_{\text{cat}}^{(3)}$, $\tilde{v}_{\text{ca}}^{(2)} v_t$, & $v_c \tilde{v}_{\text{at}}^{(2)}$ via P_n 's. We exploit this in the following sections.

3.2 Left-Inference via Retokenization

To perform left-inference—predicting the *initial* token of a word given trailing context—we retokenize the energy function into a left-gauge form. For each layer n , the hierarchical Hopfield model learns 2-point correlations of the form:

$$H_n = \sum_{\mu_{n-1}, k} g_{\mu_{n-1}, k}^{(n)} \tilde{v}_{\mu_{n-1}}^{(n-1)} v_k, \quad (8)$$

where $\tilde{v}^{(n-1)}$ is the projected trailing context, and v_k is the final (predicted) token. This is the default right-inference form.

To express H_n in a form suitable for left-inference, we apply the left-tokenized projector $P_{L,n}^{\mu_n, j, \mu_{n-1}}$, defined recursively via:

$$\tilde{v}_{\mu_n}^{(n)} = \sum_{j, \mu_{n-1}} P_{L,n}^{\mu_n, j, \mu_{n-1}} v_j \tilde{v}_{\mu_{n-1}}^{(n-1)}. \quad (9)$$

The energy becomes:

$$H_n = \sum_{\mu_n} g_{\mu_n}^{(n)} \tilde{v}_{\mu_n}^{(n)} = \sum_{j, \mu_{n-1}, \mu_n} g_{\mu_n}^{(n)} P_{L,n}^{\mu_n, j, \mu_{n-1}} v_j \tilde{v}_{\mu_{n-1}}^{(n-1)}. \quad (10)$$

To compute the gradient for left-inference, we differentiate with respect to the initial token v_j :

$$\frac{\partial H}{\partial v_j} = \sum_{n \geq 2} \sum_{\mu_{n-1}, \mu_n} g_{\mu_n}^{(n)} P_{L,n}^{\mu_n, j, \mu_{n-1}} \tilde{v}_{\mu_{n-1}}^{(n-1)}. \quad (11)$$

This is structurally symmetric to the right-inference form:

$$\frac{\partial H}{\partial v_k} = \sum_{n \geq 2} \sum_{\mu_{n-1}, k} g_{\mu_{n-1}, k}^{(n)} \tilde{v}_{\mu_{n-1}}^{(n-1)}, \quad (12)$$

but now uses the left-retokenized projector and reversed token ordering.

3.3 Example: Learning from dogs, cats, and frogs

To illustrate how the hierarchical Hopfield model builds structure from scratch, we walk through the learning process for a minimal training set consisting of three words:

dogs, cats, frog.

We assume the model begins with a basis token set of dimension $d = 26$, one for each letter of the English alphabet: $v_j \in \{v_a, \dots, v_z\}$. The model learns from co-occurrence patterns in the training data, using local Hebbian updates following Eqn 1.

Step 1: Learning Bigrams

From the three words, the following bigrams (2-grams) occur:

do, og, gs, ca, at, ts, fr, ro, og.

The model defines a projection tensor $P_2^{\mu_2, j_1, j_2}$, with a separate index μ_2 for each learned bigram:

$$P_2 = \sum_{\mu_2} P_2^{\mu_2, j_1, j_2} \tilde{v}_{\mu_2}^{(2)} v_{j_1} v_{j_2},$$

where $P_2^{\mu_2, j_1, j_2} = 1$ for each bigram above. These define eight new 2-gram tokens:

$$\tilde{v}_{\text{do}}^{(2)}, \tilde{v}_{\text{og}}^{(2)}, \tilde{v}_{\text{gs}}^{(2)}, \tilde{v}_{\text{ca}}^{(2)}, \tilde{v}_{\text{at}}^{(2)}, \tilde{v}_{\text{ts}}^{(2)}, \tilde{v}_{\text{fr}}^{(2)}, \tilde{v}_{\text{ro}}^{(2)}.$$

Step 2: Learning Trigrams

The trigrams (3-grams) in the words are:

dog, ogs, cat, ats, fro, rog.

From the smooth bigrams above, the model constructs a new projector:

$$P_3^{\mu_3, \mu_2, j_3} = 1 \quad \text{for learned combinations} \quad \tilde{v}_{\mu_3}^{(3)} = \tilde{v}_{\mu_2}^{(2)} v_{j_3}.$$

This yields six smooth trigram tokens:

$$\tilde{v}_{\text{dog}}^{(3)}, \tilde{v}_{\text{ogs}}^{(3)}, \tilde{v}_{\text{cat}}^{(3)}, \tilde{v}_{\text{ats}}^{(3)}, \tilde{v}_{\text{fro}}^{(3)}, \tilde{v}_{\text{rog}}^{(3)}.$$

Step 3: Learning 4-grams (Full Words)

Finally, the full words **dogs, cats, and frog** are learned:

$$\begin{aligned} \tilde{v}_{\text{dog}}^{(3)} v_s &\Rightarrow \tilde{v}_{\text{dogs}}^{(4)}, & \tilde{v}_{\text{cat}}^{(3)} v_s &\Rightarrow \tilde{v}_{\text{cats}}^{(4)}, \\ \tilde{v}_{\text{fro}}^{(3)} v_g &\Rightarrow \tilde{v}_{\text{frog}}^{(4)}. \end{aligned}$$

Summary: Smooth Tokenset

After training, the smooth tokenset contains:

- 8 bigrams: $\tilde{v}_{\text{do}}^{(2)}, \tilde{v}_{\text{og}}^{(2)}, \tilde{v}_{\text{gs}}^{(2)}, \tilde{v}_{\text{ca}}^{(2)}, \tilde{v}_{\text{at}}^{(2)}, \tilde{v}_{\text{ts}}^{(2)}, \tilde{v}_{\text{fr}}^{(2)}, \tilde{v}_{\text{ro}}^{(2)}$
- 6 trigrams: $\tilde{v}_{\text{dog}}^{(3)}, \tilde{v}_{\text{ogs}}^{(3)}, \tilde{v}_{\text{cat}}^{(3)}, \tilde{v}_{\text{ats}}^{(3)}, \tilde{v}_{\text{fro}}^{(3)}, \tilde{v}_{\text{rog}}^{(3)}$
- 3 4-grams: $\tilde{v}_{\text{dogs}}^{(4)}, \tilde{v}_{\text{cats}}^{(4)}, \tilde{v}_{\text{frog}}^{(4)}$

Final Projectors

The learned projectors take the form:

$$\begin{aligned}
 P_2^{\mu_2, j_1, j_2} &= 1 \quad \text{for } (\mu_2, j_1, j_2) \in \{(\text{do}, \text{d}, \text{o}), (\text{og}, \text{o}, \text{g}), (\text{gs}, \text{g}, \text{s}), (\text{ca}, \text{c}, \text{a}), \\
 &\quad (\text{at}, \text{a}, \text{t}), (\text{ts}, \text{t}, \text{s}), (\text{fr}, \text{f}, \text{r}), (\text{ro}, \text{r}, \text{o})\} \\
 P_3^{\mu_3, \mu_2, j_3} &= 1 \quad \text{for } (\mu_3, \mu_2, j_3) \in \{(\text{dog}, \text{dog}), (\text{ogs}, \text{og}, \text{s}), (\text{cat}, \text{cat}), \\
 &\quad (\text{ats}, \text{at}, \text{s}), (\text{fro}, \text{fr}, \text{o}), (\text{rog}, \text{ro}, \text{g})\} \\
 P_4^{\mu_4, \mu_3, j_4} &= 1 \quad \text{for } (\mu_4, \mu_3, j_4) \in \{(\text{dogs}, \text{dog}, \text{s}), (\text{cats}, \text{cat}, \text{s}), (\text{frog}, \text{fro}, \text{g})\}
 \end{aligned} \tag{13}$$

Or equivalently written as a superposition of tensor product states (a.k.a an **entangled** state [53]):

$$\begin{aligned}
 P_2 &= \tilde{v}_{\text{do}}^{(2)} v_{\text{d}} v_{\text{o}} + \tilde{v}_{\text{og}}^{(2)} v_{\text{o}} v_{\text{g}} + \tilde{v}_{\text{gs}}^{(2)} v_{\text{g}} v_{\text{s}} + \tilde{v}_{\text{ca}}^{(2)} v_{\text{c}} v_{\text{a}} + \tilde{v}_{\text{at}}^{(2)} v_{\text{a}} v_{\text{t}} \\
 &\quad + \tilde{v}_{\text{ts}}^{(2)} v_{\text{t}} v_{\text{s}} + \tilde{v}_{\text{fr}}^{(2)} v_{\text{f}} v_{\text{r}} + \tilde{v}_{\text{ro}}^{(2)} v_{\text{r}} v_{\text{o}} \\
 P_3 &= \tilde{v}_{\text{dog}}^{(3)} \tilde{v}_{\text{do}}^{(2)} v_{\text{g}} + \tilde{v}_{\text{ogs}}^{(3)} \tilde{v}_{\text{og}}^{(2)} v_{\text{s}} + \tilde{v}_{\text{cat}}^{(3)} \tilde{v}_{\text{ca}}^{(2)} v_{\text{t}} + \tilde{v}_{\text{ats}}^{(3)} \tilde{v}_{\text{at}}^{(2)} v_{\text{s}} \\
 &\quad + \tilde{v}_{\text{fro}}^{(3)} \tilde{v}_{\text{fr}}^{(2)} v_{\text{o}} + \tilde{v}_{\text{rog}}^{(3)} \tilde{v}_{\text{ro}}^{(2)} v_{\text{g}} \\
 P_4 &= \tilde{v}_{\text{dogs}}^{(4)} \tilde{v}_{\text{dog}}^{(3)} v_{\text{s}} + \tilde{v}_{\text{cats}}^{(4)} \tilde{v}_{\text{cat}}^{(3)} v_{\text{s}} + \tilde{v}_{\text{frog}}^{(4)} \tilde{v}_{\text{fro}}^{(3)} v_{\text{g}}
 \end{aligned} \tag{16}$$

We can understand the product of projector tensors $P_n P_{n-1} \cdots P_2$ as encoding a bundle of finite state transitions (or feature maps), e.g $v_{\text{r}} \rightarrow \tilde{v}_{\text{fr}}^{(2)} \rightarrow \tilde{v}_{\text{fro}}^{(3)} \rightarrow \tilde{v}_{\text{frog}}^{(4)}$, which collectively describe all possible paths toward the terminal nodes of the DAG.

Every token in this hierarchy is retokenizable into only previously learned parts. This guarantees that inference can recursively decompose any learned token, and that the vocabulary is self-consistent and locally compositional. For example, given context **frog**, the model knows to terminate right-inference because no merger of $\tilde{v}_{\text{frog}}^{(4)}$ with another token exists as a feature map – defined by non-vanishing action of $P_n P_{n-1} \cdots P_2$ (e.g Fig 1). Nevertheless, the model can still infer **frogs** as the best non-smooth construction due to local interactions $g_{\text{og}}^{(2)}$ & $g_{\text{ogs}}^{(3)}$.

This latter subtlety highlights the hybrid sub-symbolic/automaton nature of the model, where tokenization² plays a dynamical role during inference to determine boundaries, and therefore imbues the model with a notion of *accepted* string akin to automata. In energetic terms, the accepted strings live in a low-energy manifold (the smooth tokenset), and therefore are the most-likely configurations to be observed given the context. We may therefore think of the automaton as living in the ground state, with its language being the ground state configurations [49]. This approximate behavior is made precise by the introduction of projectors (and therefore a consequence of learning higher-order correlations while requiring locality).

²This dynamic tokenization is distinct from both tokenization [16, 55] & entropy-based approaches to LLM’s [2, 37, 58, 69]. LLM’s assume pretokenized input [16, 43, 55].

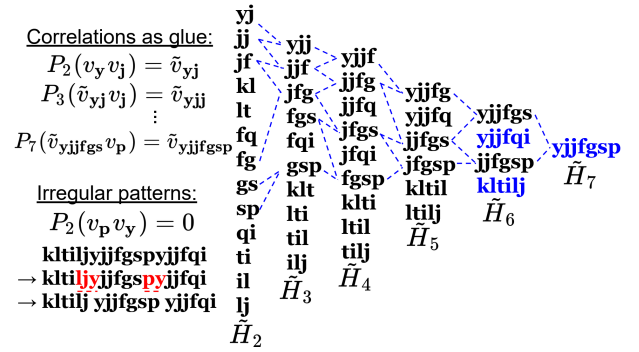


Figure 1: Summarizing the relationship between tokenizability, locality, and hierarchy. Three words from a random language [14] (shown in blue): yjifqi, kltijl, & yjifgsp.

4 THE BENEFITS OF THINKING ABOUT IT

The hierarchical short-term memory stores learned words as smooth tokens encoded via a bundle of entangled feature maps ($P_n \cdots P_2$) and local interactions ($g^{(n)}$). This allows for the model to determine word boundaries (Fig 1), as well as retrieve words from context.

However, this places a number of limitations which limit its scalability. First, it learns all feature maps as entangled, regardless of if they share overlapping graphs – this is highly impractical³. Further, word length is finite – stored strings are limited to regular-language-like structure.

The model overcomes these limitations by employing a thinking-like process we call *replay relearning*. This procedure binds the distributed features of a token sequence (e.g a word object) into a new long-term embedding neuron a_α , thus disentangling the feature maps into a series of smaller word-specific feature maps. These can later participate in inference independent of the original $g^{(n)}$ (which can be forgotten).

4.1 The Replay Game (Model Thinking)

Replay begins by selecting a random basis token v_k as seed. From this seed, the short-term memory network performs left and right inference using only the local energy gradients from $g^{(n)}$. Inference proceeds recursively: the next token v is selected based on the energy gradient

$$\Delta v_k = \sum_{n, \mu_{n-1}} g_{\mu_{n-1}, k}^{(n)} \tilde{v}_{\mu_{n-1}}^{(n-1)},$$

and sampling $\rho_k(f_k(\Delta v_k))$. At each step, retokenization ensures that only smooth (i.e compositional) features are activated.

The process continues until the inferred string reaches a natural boundary – a region where no further smooth retokenization is possible. The result is a spontaneously generated word, such as:

$$[v_c, v_a, v_t, v_s].$$

³Because the feature maps are entangled, the projector size scales as the square of the number of learned features (n -grams) [14]. Because the P_n are sparse, a tradeoff can be made to improve memory, however at the cost of losing the representational power of dense matrices. Additionally, memories would have to be stored & accessed from a singular large hierarchy, regardless of whether most of the memory traces are unrelated to the given context. And we noticed the total number of n -grams in a real text scales as a power-law [14].

At some point during this replay cycle — whether mid-replay or post-hoc — we introduce a new auxiliary neuron a_α from an external source (conceptually, a pool at infinity). We activate it by construction (i.e we force it to fire).

As the replay proceeds, the features $\tilde{v}^{(n)}$ that fire over time become locally Hebbian-correlated with the firing a_α . That is, at each replay step, the memory weight is updated by:

$$m_{\alpha,\mu_n}^{(n)} \leftarrow m_{\alpha,\mu_n}^{(n)} + \eta a_\alpha \tilde{v}_{\mu_n}^{(n)},$$

where η is a learning rate.

Alternatively — and equivalently — one can view the full word replay as producing a batch of active features, which are then bound in a single step to the new a_α neuron. It encodes the feature content across all n -gram layers of the retokenization hierarchy:

$$\text{e.g. } a_\alpha = \text{cats} \leftrightarrow \{v_c, v_a, v_t, v_s, \tilde{v}_{ca}^{(2)}, \tilde{v}_{at}^{(2)}, \tilde{v}_{ts}^{(2)}, \tilde{v}_{cat}^{(3)}, \tilde{v}_{ats}^{(3)}, \tilde{v}_{cats}^{(4)}\}.$$

The result is a key-value memory binding [4, 18, 62]: the neuron a_α becomes a long-term embedding associated with the full replayed word. Over time, this mechanism constructs a library of **long-term memory** neurons $\{a_\alpha\}$, each associated with a unique word and its compositional features. Once learned, these embeddings enable fast inference via pattern completion: a partial word (e.g. a suffix or prefix) can trigger an embedding, which drives next-token prediction.

Benefits of Replay Relearning.

- **Compression:** Word features are projected onto low-rank memory vectors.
- **Decoupling:** Embeddings allow hierarchical memory $g^{(n)}$ to be forgotten or reused.
- **Continual Learning:** New embeddings can be learned without overwriting existing ones.
- **Parallelism:** Each a_α contributes independently to inference.
- **Emergent Computation:** The a_α contribution to inference generalizes beyond local n -gram statistics.

5 EMERGENT HIERARCHICAL KEY-VALUE MEMORY (RECOGNITION)

Inference proceeds as a sequence of discrete event updates. At each time step, a new token is predicted based on the trailing context through the structure stored in both short-term ($g^{(n)}$) and long-term ($m^{(n)}$) memory. The full Hamiltonian is therefore

$$H = \sum_n \sum_{\mu_{n-1}, k} g_{\mu_{n-1}, k}^{(n)} \tilde{v}_{\mu_{n-1}}^{(n-1)} v_k + \sum_\alpha a_\alpha \left(\sum_n \sum_{\mu_n} m_{\alpha, \mu_n}^{(n)} \tilde{v}_{\mu_n}^{(n)} \right). \quad (17)$$

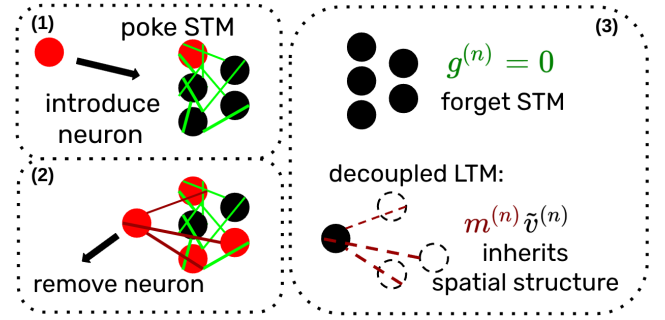
5.1 Update Logic

Each token prediction is based on evaluating local gradients:

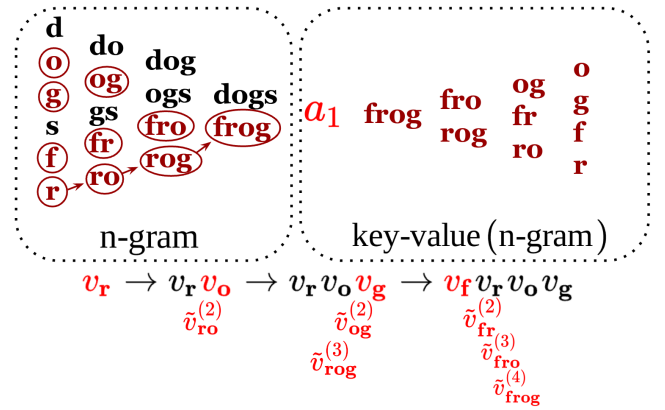
$$Q \leftarrow f_Q(\Delta Q), \quad \Delta Q := \frac{\partial H}{\partial Q}, \quad (18)$$

for $Q \in \{v_k, a_\alpha\}$, where f_Q is any bounded activation function.

We choose to update a_α neurons first. Their updated values are then used to compute the update for v_k . The corresponding



(a) The dynamic game of “replay”: (1) Randomly activate node in short-term memory (STM). (2) Introduce new neuron until hierarchy converges on stored memory, then remove it. (3) Added neurons emerge as long-term memory (LTM).



(b) LEFT: State-transitions of the STM converge on terminal node. Red shows features activated during replay. RIGHT: Embedding neuron (a_1) learns an emergent hierarchical key-value memory, which is an attention mechanism wrapped around a word-specific n -gram model. BOTTOM: Replay as autoregression with boundary awareness. Red shows activated trailing context tokens.

Figure 2: Dynamically Coding the Local Plastic Structure

gradients are:

$$\Delta a_\alpha = \sum_n \sum_{\mu_n} m_{\alpha, \mu_n}^{(n)} \tilde{v}_{\mu_n}^{(n)}, \quad (19)$$

$$\Delta v_k = \sum_n \sum_{\mu_{n-1}} \left(g_{\mu_{n-1}, k}^{(n)} + \sum_\alpha a_\alpha m_{\alpha, \mu_{n-1}, k}^{(n)} \right) \tilde{v}_{\mu_{n-1}}^{(n-1)}. \quad (20)$$

5.2 Key-Value Memory via Fast Embedding Neurons

If a_α neurons respond more rapidly than v_k , we treat them as reaching a fixed point first [32]:

$$a_\alpha = f_\alpha \left(\sum_n \sum_{\mu_n} m_{\alpha, \mu_n}^{(n)} \tilde{v}_{\mu_n}^{(n)} \right). \quad (21)$$

Plugging into the equation for Δv_k yields:

$$\Delta v_k = \sum_n \sum_{\mu_{n-1}} g_{\mu_{n-1},k}^{(n)} \tilde{v}_{\mu_{n-1}}^{(n-1)} \quad (22)$$

$$+ \sum_{\alpha} f_{\alpha} \left(\sum_{n'} \sum_{\mu_{n-1}'} m_{\alpha, \mu_{n-1}'}^{(n')} \tilde{v}_{\mu_{n-1}'}^{(n')} \right) \cdot \sum_n \sum_{\mu_{n-1}} m_{\alpha, \mu_{n-1}, k}^{(n)} \tilde{v}_{\mu_{n-1}}^{(n-1)}. \quad (23)$$

Eqn 23 defines a **hierarchical key-value memory**, where:

- The *key* is the set of smooth projected context tokens $\tilde{v}^{(n)}$,
- The *embedding neuron* a_{α} is selected by the context via $f_{\alpha}(\cdot)$,
- The *value* is the distribution over next tokens v_k , computed via the activated embedding.

This emergent key-value memory mechanism allows long-term associations to be built from local dynamics alone, forming the basis for structured retrieval and generalization in later inference. Thus the model can generalize beyond local n -gram statistics, enabling long-range coherence, partial match inference, and efficient lookup. We refer to this process as *recognition*⁴.

5.2.1 Key-Value Memory Example. Consider Eqn 23 with $g^{(n)} = 0$, s.t inference is driven purely by a_{α} . Suppose we have two learned word embeddings, $\alpha \in \{1, 2\}$, corresponding to:

$$a_1 \leftrightarrow \mathbf{cats}, \quad a_2 \leftrightarrow \mathbf{dogs}.$$

Then the update becomes:

$$\begin{aligned} \Delta v_k = & f_1 \left(\tilde{v}_{ca}^{(2)} m_{1,ca}^{(2)} + \tilde{v}_{at}^{(2)} m_{1,at}^{(2)} + \tilde{v}_{cat}^{(3)} m_{1,cat}^{(3)} + \tilde{v}_{ats}^{(3)} m_{1,ats}^{(3)} + \tilde{v}_{cats}^{(4)} m_{1,cats}^{(4)} \right) \\ & \times \left(\tilde{v}_{ca}^{(2)} m_{1,ca,k}^{(3)} + \tilde{v}_{at}^{(2)} m_{1,at,k}^{(3)} + \tilde{v}_{cat}^{(3)} m_{1,cat,k}^{(4)} \right) \\ & + f_2 \left(\tilde{v}_{do}^{(2)} m_{2,do}^{(2)} + \tilde{v}_{og}^{(2)} m_{2,og}^{(2)} + \tilde{v}_{dog}^{(3)} m_{2,dog}^{(3)} + \tilde{v}_{ogs}^{(3)} m_{2,ogs}^{(3)} + \tilde{v}_{dogs}^{(4)} m_{2,dogs}^{(4)} \right) \\ & \times \left(\tilde{v}_{do}^{(2)} m_{2,do,k}^{(3)} + \tilde{v}_{og}^{(2)} m_{2,og,k}^{(3)} + \tilde{v}_{dog}^{(3)} m_{2,dog,k}^{(4)} \right). \quad (24) \end{aligned}$$

Note that generically $m_{\alpha,k}^{(1)}$ (monogram) terms also contribute, but we suppress them in this example to preserve space.

If the context consists of v_a, v_t , then $\tilde{v}_{at}^{(2)} = 1$ and all other projections vanish. The update reduces to:

$$\Delta v_k = f_1(m_{1,at}^{(2)}) \cdot m_{1,at,k}^{(3)}.$$

This predicts the next token v_k with the strongest overlap with s , due to the binding $m_{1,at,k}^{(3)} = m_{1,ats}^{(3)} \delta_{k,s}$.

Note that the update of a_{α} inherits information about morphological structure (the projection maps) from its interaction with the $\tilde{v}^{(n)}$. Thus, smooth features in the context trigger the appropriate word embedding via $f_{\alpha}(\cdot)$, which then drives prediction through projection maps. Thus there is no need to further encode positional relationships, which is handled by the projectors. We discuss

⁴Note that *recognition* can interfere with *tokenization*. For instance, the repeated string formed from **monk+eye**, i.e **...onkeyemonkeyemon...**, uniquely tokenizes back into the two words stated, however, the reader may still recognize **monkey** or **key** even though they don't uniquely tokenize the string, highlighting the competition between fast long-term memory effects with slower tokenizing short-term memory [14].

how this inheritance allows optimizing for word-specific projection maps in the following section.

5.3 Compression via Word-Specific Projector Decomposition

To illustrate how replay leads to compression, we begin with a concrete example. Suppose the model has learned the following projectors:

Bigrams:

$$P_2 = \tilde{v}_{ca}^{(2)} v_c v_a + \tilde{v}_{at}^{(2)} v_a v_t + \tilde{v}_{ts}^{(2)} v_t v_s + \tilde{v}_{do}^{(2)} v_d v_o + \tilde{v}_{og}^{(2)} v_o v_g + \tilde{v}_{gs}^{(2)} v_g v_s \quad (25)$$

Trigrams:

$$P_3 = \tilde{v}_{cat}^{(3)} \tilde{v}_{ca}^{(2)} v_t + \tilde{v}_{ats}^{(3)} \tilde{v}_{at}^{(2)} v_s + \tilde{v}_{dog}^{(3)} \tilde{v}_{do}^{(2)} v_g + \tilde{v}_{ogs}^{(3)} \tilde{v}_{og}^{(2)} v_s \quad (26)$$

4-grams:

$$P_4 = \tilde{v}_{cats}^{(4)} \tilde{v}_{cat}^{(3)} v_s + \tilde{v}_{dogs}^{(4)} \tilde{v}_{dog}^{(3)} v_s \quad (27)$$

Now consider the replay-imprinted m -tensors for $\alpha = \mathbf{cats}$:

$$\begin{aligned} m_{cats}^{(2)} &= \tilde{v}_{ca}^{(2)} + \tilde{v}_{at}^{(2)} + \tilde{v}_{ts}^{(2)}, \\ m_{cats}^{(3)} &= \tilde{v}_{cat}^{(3)} + \tilde{v}_{ats}^{(3)}, \\ m_{cats}^{(4)} &= \tilde{v}_{cats}^{(4)}. \end{aligned} \quad (28)$$

We now demonstrate compression by contracting $m_{cats}^{(3)}$ with the entangled projector P_3 :

$$\begin{aligned} m_{cats}^{(3)} P_3 &= (\tilde{v}_{cat}^{(3)} + \tilde{v}_{ats}^{(3)}) (\tilde{v}_{cat}^{(3)} \tilde{v}_{ca}^{(2)} v_t + \tilde{v}_{ats}^{(3)} \tilde{v}_{at}^{(2)} v_s \\ &+ \tilde{v}_{dog}^{(3)} \tilde{v}_{do}^{(2)} v_g + \tilde{v}_{ogs}^{(3)} \tilde{v}_{og}^{(2)} v_s) \\ &= \tilde{v}_{ca}^{(2)} v_t + \tilde{v}_{at}^{(2)} v_s, \end{aligned} \quad (29)$$

where orthogonality eliminates the contributions from tokens unrelated to **cats**. The result is a disentangled, word-specific tensor chain:

$$= (\tilde{v}_{cat}^{(3)} + \tilde{v}_{ats}^{(3)}) (\tilde{v}_{cat}^{(3)} \tilde{v}_{ca}^{(2)} v_t + \tilde{v}_{ats}^{(3)} \tilde{v}_{at}^{(2)} v_s) := \hat{m}_{cats}^{(3)} \hat{P}_3^{cats}. \quad (30)$$

This procedure can be recursively applied to the full projector chain $P_3 P_2$ to yield a compressed set of projectors \hat{P}_n^{α} for each word α . These retain only the subspaces relevant to α , enabling scalable and disentangled memory representations.

Next, we generalize this process to arbitrary word embeddings using SVD-based decomposition of the m -capped projection chains.

5.4 Generalized Compression via Projector Contraction

The concrete example above illustrates how word-specific projector chains can be disentangled by pruning irrelevant branches. We now formalize this procedure using a sequence of algebraic contractions and SVDs [22, 42, 53], resulting in a compressed representation of the hierarchical projector chain for each word embedding.

We begin with the full replay expression for a given word embedding a_α :

$$\sum_{\mu_n} m_{\alpha, \mu_n}^{(n)} \tilde{v}_{\mu_n}^{(n)} = \sum_{\mu_n, \mu_{n-1}, \dots, \mu_2} m_{\alpha, \mu_n}^{(n)} P_n^{\mu_n, \mu_{n-1}, j_n} \dots P_2^{\mu_2, j_1, j_2} v_{j_1} v_{j_2} \dots v_{j_n}. \quad (31)$$

This expression can be interpreted as a long chain of projection maps contracted with the memory vector $m_\alpha^{(n)}$ at the top. In practice, many components of $m_\alpha^{(n)}$ will be zero, as the embedding stores only features observed during the replay of word α .

To compress this representation, we apply a sequence of SVD decompositions layer by layer. First, we perform an SVD of the capped tensor:

$$m_{\alpha, \mu_n}^{(n)} = \sum_{\beta_n} \hat{m}_{\alpha, \beta_n}^{(n)} V_n^{\beta_n, \mu_n}, \quad (32)$$

where V_n defines a word-specific low-rank subspace over μ_n , and $\hat{m}_{\alpha, \beta_n}^{(n)}$ is the compressed top cap.

Next, we contract V_n with P_n :

$$\tilde{P}_n^{\beta_n, \mu_{n-1}, j_n} = \sum_{\mu_n} V_n^{\beta_n, \mu_n} P_n^{\mu_n, \mu_{n-1}, j_n}. \quad (33)$$

This new projector has reduced dimension, containing only n -grams relevant to a_α . We then reshape this tensor into a matrix over index pairs (μ_{n-1}, j_n) and perform another SVD: $\tilde{P}_n^{\beta_n, (\mu_{n-1}, j_n)} = \sum_{\omega} U_n^{\beta_n, \omega} D_n^{\omega, (\mu_{n-1}, j_n)} V_n^{\omega, (\mu_{n-1}, j_n)}$.

We now proceed to compress the next layer. We contract the decomposed V from above with the next projector:

$$T_{\omega, j_n, \mu_{n-2}, j_{n-1}} = \sum_{\mu_{n-1}} V_n^{\omega, \mu_{n-1}, j_n} P_{n-1}^{\mu_{n-1}, \mu_{n-2}, j_{n-1}}. \quad (34)$$

Merging the left and right index pairs, we perform another decomposition: $T_{(\omega, j_n), (\mu_{n-2}, j_{n-1})} = \sum_{\beta_{n-1}} U'_{(\omega, j_n), \beta_{n-1}} D'_{\beta_{n-1}, (\mu_{n-2}, j_{n-1})}$. We now define the fully compressed projector:

$$\hat{P}_n^{\beta_n, \beta_{n-1}, j_n} = \sum_{\omega} U_n^{\beta_n, \omega} U'_{\omega, j_n, \beta_{n-1}} D'_{\beta_{n-1}}, \quad (35)$$

$$\tilde{P}_{n-1}^{\beta_{n-1}, \mu_{n-2}, j_{n-1}} = V'_{\beta_{n-1}, \mu_{n-2}, j_{n-1}}. \quad (36)$$

We repeat this contraction-decomposition process recursively, defining new compressed projection maps \hat{P}_n and reduced intermediate indices $\beta_{n-1}, \beta_{n-2}, \dots$ at each step.

The final expression for the replayed memory becomes:

$$\sum_{\beta_n, \dots, \beta_2} \hat{m}_{\alpha, \beta_n}^{(n)} \hat{P}_n^{\beta_n, \beta_{n-1}, j_n} \dots \hat{P}_2^{\beta_2, j_1, j_2} v_{j_1} v_{j_2} \dots v_{j_n}. \quad (37)$$

This compressed chain retains only the information needed to reconstruct the replay trajectory of word α , eliminating all unrelated feature branches. The compression is exact if no finite SVD eigenvalues are discarded. Thus this naturally generalizes to approximate compressions via truncating irrelevant contributions to the SVD spectra. We leave this latter point for future discovery.

Benefits. This word-specific decomposition achieves two goals:

- **Disentanglement:** Removes unrelated replay trajectories (an exact compression).
- **Compression:** Optimizes the dimension of projection maps; & can regulate embedding dimension (approx).

5.5 Super-Hierarchical Key-Value Memory

The hierarchical key-value memory mechanism naturally extends to higher levels of abstraction. Just as short-term memory tokens $\tilde{v}^{(n)}$ are bound into long-term word embeddings a_α via replay, the embeddings themselves may form higher-order structures, such as phrases, idioms, or conceptual clusters. We introduce a second memory hierarchy built on projected embedding neurons $\tilde{a}^{(m)}$, with feature maps \mathcal{P}_m , correlation weights $G^{(m)}$, and memory tensors $M^{(m)}$. This forms a *super-hierarchical memory*, enabling compositional inference over learned embedding structures.

To support compositional memory beyond single-word representations, we extend the Hamiltonian to include higher-level interactions among embedding neurons:

$$H = \sum_n \sum_{\mu_{n-1}, k} g_{\mu_{n-1}, k}^{(n)} \tilde{v}_{\mu_{n-1}}^{(n-1)} v_k + \sum_\alpha a_\alpha \left(\sum_n \sum_{\mu_n} m_{\alpha, \mu_n}^{(n)} \tilde{v}_{\mu_n}^{(n)} \right) + \sum_m \sum_{\alpha_{m-1}, \alpha} G_{\alpha_{m-1}, \alpha}^{(m)} \tilde{a}_{\alpha_{m-1}}^{(m-1)} a_\alpha + \sum_\xi b_\xi \left(\sum_m \sum_{\alpha_m} M_{\xi, \alpha_m}^{(m)} \tilde{a}_{\alpha_m}^{(m)} \right), \quad (38)$$

where a_α are embedding neurons and b_ξ are super-embedding neurons. Feature projections $\tilde{v}^{(n)}$ and $\tilde{a}^{(m)}$ are defined via retokenization hierarchies P_n and \mathcal{P}_m respectively.

Update Logic: We compute gradients

$$\Delta v_k = \frac{\partial H}{\partial v_k}, \quad \Delta a_\alpha = \frac{\partial H}{\partial a_\alpha}, \quad \Delta b_\xi = \frac{\partial H}{\partial b_\xi}, \quad (39)$$

and apply bounded updates: $Q \leftarrow f_Q(\Delta Q)$ for $Q \in \{v_k, a_\alpha, b_\xi\}$. We treat b_ξ & a_α as being faster than v_k (i.e hierarchy of equilibration times $\tau_b \ll \tau_a \ll \tau_v$ [32, 33]). Thus we solve for b_ξ and a_α first, then substitute into Δv_k .

Inference Equation: Letting $g^{(n)} = G^{(m)} = 0$, we derive the inference rule:

$$\Delta v_k = \sum_\alpha f_\alpha \left(\sum_{n'} \sum_{\mu_{n'}} m_{\alpha, \mu_{n'}}^{(n')} \tilde{v}_{\mu_{n'}}^{(n')} + \sum_\xi f_\xi \left(\sum_{m'} \sum_{\alpha_{m'}} M_{\xi, \alpha_{m'}}^{(m')} \tilde{a}_{\alpha_{m'}}^{(m')} \right) \times \sum_{\alpha_{m-1}} M_{\xi, \alpha_{m-1}, \alpha}^{(m)} \tilde{a}_{\alpha_{m-1}}^{(m-1)} \right) \sum_n \sum_{\mu_{n-1}, k} m_{\alpha, \mu_{n-1}, k}^{(n)} \tilde{v}_{\mu_{n-1}}^{(n-1)}. \quad (40)$$

This defines a *super-hierarchical key-value memory*: the context selects a super-embedding b_ξ , which activates relevant embeddings a_α , which in turn retrieve fine-grained retokenized features for predicting v_k .

5.5.1 Plasticity, Emergence, and the role of Space & Time.

The emergent key-value memories discussed here are a consequence of the plastic nature of Hebbian learning, combined with the hierarchical tokenizing inference. These new mechanisms are not put in by hand – there is no “key-value memory layer” added to the system – and no retraining of the entire model is necessary. Instead, introducing a single new neuron to the system is sufficient in order for them to arise, demonstrating that they are truly *emergent* structures. (Nor is explicit data necessary – see Discussion.)

This type of plasticity is not present in models which learn via optimizing a global objective (back propagation). While such models are typically modular, their architecture is fixed beforehand. Though the black box paradigm permits a type of data-driven “emergence”, it is not the type of structural emergence described here, but instead reflects a discovery of internal representations allowed within the fixed architecture. The attention mechanism of an LLM is *assumed* beforehand [63], not a learned structure. This differs from Conway’s Game of Life, which can “learn” a Turing machine – not from recognizing patterns in data nor minimizing an objective, but as an accident due to the local dynamics & initial conditions [50, 51].

The hierarchical key-value memories described here can be understood as arising due to the interplay of space & time. The spatial aspect is reflected in how the key-value relationship preserves the morphological structure, such that the value part encodes how to complete a word from a triggered key. Thus no positional embeddings are necessary (or helpful). This spatial awareness is learned because retokenization makes replay boundary aware; so that the added embedding neuron correlates with the features corresponding to smoothly correlated regions of string. By having the neuron activated throughout this cycle, it learns this smooth feature set as if all its elements fired *simultaneously* during a single Hebbian update step. At face value this process is “precisely timed”, but thanks to the spatial awareness of retokenization, doing this precise timing is trivial.

It’s useful to think of replay as a minimally structured game (or a local dynamic coding scheme) – grab a new neuron, poke short-term memory to randomly replay its correlations, then repeat the process again with a new neuron once replay terminates. It works because the local event learning makes continued learning & emergence incidental. The assumed structure of replay is chosen to exploit this “accidental learning”. Likely other (more efficient less random) structured games exists which exploit this accident.

Even following our minimal replay blueprint, the number of possible different emergent structures grows combinatorially with the number of learned long-term embeddings. As more embedding neurons populate the long-term memory ($V_\Omega := (v_k, a_\alpha, b_\xi, \dots)_\Omega$), the model can learn correlations between these embeddings ($V_\Omega V_{\Omega'}$ for subset of Ω), which can then form entirely novel compositional structures (beyond hierarchical & super-hierarchical). These newly learned structures, in turn, enrich the token representations available to short-term memory, enabling further complexity. Classifying all possible emergent structures, given the local dynamics, is akin to exactly solving a physics problem. In general this is not always possible, but nevertheless opens a potentially fruitful direction for future research.

6 TOY EXAMPLE: FINGER COUNTING

This example illustrates how replay and hierarchical memory enable the model to bind structured inputs (e.g. finger gestures) to symbolic tokens (e.g. number words).

6.1 Modalities and Embeddings

We assume two input modalities:

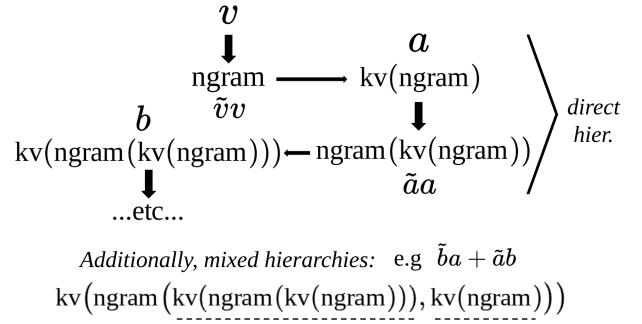


Figure 3: Hierarchies of hierarchies: STM’s are n-gram models which build features ($\tilde{v}, \tilde{a}, \tilde{b}, \dots$) from relevant correlations ($\tilde{v}, \tilde{a}, \dots$). These can be replayed into symbolic key-value memory tokens of increasing complexity LTM (a, b, \dots). We show the emergent inference classes learned at each step. In addition to the direct hierarchies, LTM tokens of mixed class can be correlated.

- **Letter modality:** Basis tokens v_k for alphabet letters (e.g., v_o, v_n, v_e).
- **Finger modality:** Scalars $u \in \{0, 1\}$ indicating raised fingers.

Each embedding a_α is associated with hierarchical memory:

$$m_\alpha = \sum_n \sum_{\mu_n} m_{\alpha, \mu_n}^{(n)} \tilde{v}_{\mu_n}^{(n)}$$

For example, the word “one” is stored as:

$$m_1 = m_{1,o}^{(1)} v_o + m_{1,n}^{(1)} v_n + m_{1,e}^{(1)} v_e \\ + m_{1,on}^{(2)} \tilde{v}_{on}^{(2)} + m_{1,ne}^{(2)} \tilde{v}_{ne}^{(2)} + m_{1,one}^{(3)} \tilde{v}_{one}^{(3)}$$

and similarly for “two” and “three”.

Finger gestures are retokenized as:

$$\tilde{u}^{(n)} = \prod_{x=1}^n u_x,$$

with $\tilde{u}^{(n)} = 1$ if n fingers are raised.

6.2 Binding Fingers to Numbers

We define the Hamiltonian:

$$H = \sum_\alpha a_\alpha \left(\sum_n \sum_{\mu_n} m_{\alpha, \mu_n}^{(n)} \tilde{v}_{\mu_n}^{(n)} \right) \quad (41)$$

$$+ G_1^{(1)} a_1 u + G_2^{(2)} a_2 \tilde{u}^{(2)} + G_3^{(3)} a_3 \tilde{u}^{(3)}. \quad (42)$$

where the G couplings are learned via Hebbian updates, e.g. showing **two** and two raised fingers. (Technically, replay will bind $\alpha > n$ embeddings to $\tilde{u}^{(n)}$, such as a_3 being bound to u , $\tilde{u}^{(2)}$, and $\tilde{u}^{(3)}$. But this interference is mitigated by biasing $G_\alpha^{(n)} \rightarrow \beta^n G_\alpha^{(n)}$ with $\beta > 1$, and choosing f_α to be normalization.)

During inference we raise 2 fingers ($\tilde{u}^{(n)} = \sum_{n' \leq 2} \delta_{n', n}$).

$$\Delta a_\alpha = G_\alpha^{(n)} \tilde{u}^{(n)} \Rightarrow a_\alpha \mapsto \text{“two”} \Rightarrow v_k = t, w, o.$$

That is, a finger count activates the corresponding embedding, which then drives autoregressive symbol generation following the key-value relationship encoded in Eqn 41.

7 HIERARCHICAL FEATURE MIXING & RANDOM LANGUAGE

We begin by analyzing the structure of a randomly sampled vocabulary, consisting of 100 personal names (in English or Spanish) [1]. For this set, we plot the d_n distribution, where d_n counts the number of unique n -grams observed at each scale. The resulting d_n distribution follows an approximately log-normal form, with the largest n determined by the longest name in the sample.

To probe the internal structure of the learned hierarchy, we perform a game of *cut-and-regrow* (Fig 5). Specifically, we impose a cutoff n_{cut} and delete all n -gram features with $n \geq n_{\text{cut}}$, then allow the hierarchy to regrow under the smoothness constraint. This process reveals how the underlying directed acyclic graph (DAG) of features governs regrowth: surviving features at small n serve as anchoring nodes, from which higher-order structures emerge. Memory is locally organized, such that the shortest word-length scales dominate.

When cutting at $n_{\text{cut}} \gg n_{\text{peak}}$, where n_{peak} is the location of the original d_n peak, regrowth closely reproduces the original structure, introducing minimal (or no) novelty. This is because the many lower layers of the hierarchy provide strong constraints on the space of learnable regrowths.

In contrast, cutting closer to n_{peak} loosens the scale-dependent constraints, allowing novel n -grams to form. Nevertheless, even here, the surviving short-scale DAG structure continues to guide regrowth, ensuring that generated words remain smooth and morphologically coherent.

We find that though the original notion of smoothness is perfectly preserved below the cut, cutting away more of the d_n peak causes the hierarchy to begin losing its recognizable English/Spanish nature. This highlights the importance of the n_{peak} grams to language structure⁵.

Finally, if we cut at $n_{\text{cut}} = 2$, we discard *all* memory of the original names. This is the data-free regime, where growing a hierarchy generates what we refer to as a “random language” [14]. Nevertheless, growing hierarchies under the smoothness constraint still yields finite word-lengths and an approximately log-normal d_n distribution [26, 38, 66]. This shows that bounded, hierarchical morphology is an intrinsic feature of the model itself, independent of any training data, and that language structure arises naturally from smooth hierarchical learning.

Further, this behavior illustrates a key property of the model: Short-term memory structures $g^{(n)}$ behave like a dynamic *scratch board*, where hierarchical feature mixing enables creative recombination under smoothness preservation. The model’s DAG structure

⁵For $n \lesssim n_{\text{peak}}$, d_n grows approximately exponentially, with learned constraints ($g^{(n)} = 0$) pruning branches and thereby reducing the effective growth rate. For $n > n_{\text{peak}}$, the smoothness condition takes over: new tokens are permitted only if all subgrams are valid, which recursively restricts composition and causes a collapse in d_n . This collapses guarantees finite word length [14]. In formal language terms, this might be described as a consequence of the regular-language-like limitations of stored strings.

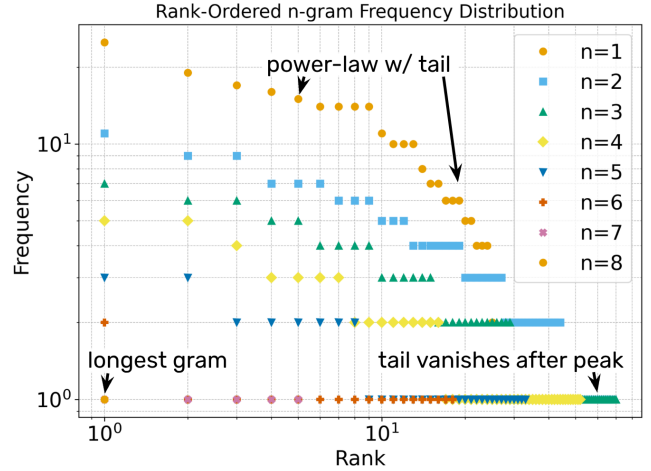


Figure 4: The frequency an n -gram (length n) appears in the vocabulary, rank-ordered from most to least frequent. The vocabulary is for the random language *bifyi* (in supplement). Equivalently, this plot can be understood as representing an effective model spectra ($g_{\text{eff}}^{(n)}$ per n). Scale-invariance emerges beyond $n_{\text{peak}} = 3$ due to the compositional structure.

naturally channels this process, enforcing compositionality while permitting exploration of new morphological forms.

7.1 Synaptic Zipf-laws

Random languages generated by our model exhibit rank-ordered n -gram frequency distributions that follow a scale-invariant Zipf-like law [17, 72], a signature of morphological structure [14]. These spectra provide insight into the statistical relevance of subword patterns, ranked from most to least frequent, and reveal how this structure scales with increasing pattern length.

Note we can interpret these ranked frequencies as defining an effective memory spectra $g_{\text{eff}}^{(n)}$, where Hebbian learning imprints frequency counts from local events \mathcal{E}_n directly into memory:

$$g_{\text{eff}}^{(n)} = \sum_{\mathcal{E}_n^{\text{vocab}}} \tilde{v}.$$

In the absence of forgetting [14], this spectrum reflects all observed correlations of length n .

Fig 4 shows the effective model spectrum corresponding to a model whose memory graph was grown randomly under the hierarchical DAG constraint. As such, the resulting distribution reflects only the inductive bias of the memory structure itself.

At short lengths ($n < n_{\text{peak}}$), constraints are minimal, and the distribution appears structureless: a Zipf-like power-law head followed by a flat tail of irrelevant n -grams, similar to those found in uniform random strings [14, 17]. However, as n increases, the DAG constraint increasingly shapes memory formation. Beyond the peak, the tail vanishes and the power-law scaling persists, signaling the emergence of a dominant compositional structure at longer lengths.

8 DISCUSSION

8.1 Where did the data come from?

Neither punctuation nor spacing are necessary elements of writing:

youcanreadthisoranytextjustfine.

This property is not special to this example, but is a general quality of human language patterns. Historically, human writing existed without specialized tokens indicating boundary. This is perhaps best illustrated by alphabets, whose fundamental tokens are meaningless beyond their sound associations. And yet such texts could (and can) still be read. This is only possible because human language is inherently *tokenizable*. There exists a statistical distinction between word-forming and non-word-forming patterns. The later introduction of spaces, punctuation, and capitalization served to mark these boundaries, but they are not themselves fundamental to the structure of language. They are external annotations for a structure already present in the stream of phonetic or orthographic symbols.

The existence of tokenizable structure in language raises a deeper question: why should such structure exist at all? Conventional language models don't address this distinction. All tokens—whether letters, spaces, punctuation, or stop tokens—are treated as elements of a single, undifferentiated vocabulary. These models assume the data has already been segmented, and that its structure reflects a meaningful set of distinctions. But this sidesteps the question of origin. The model is not responsible for discovering the structure of language, only reproducing it. By assuming the existence of a token vocabulary and training on massive amounts of pre-tokenized data, the model inherits the statistical regularities of language without explaining them. It becomes a powerful recognizer, but not a theory of how language—and its specific structure—emerges at all.

To study how such structure can emerge, we present our model with the 26 lowercase alphabetic characters as its only input features. This is not a simplification, but the intended use of the model. Learning in our framework proceeds by growing a memory structure dictated by local Hebbian updates constrained to follow a hierarchical DAG. Information is retained only when the correlations in the data align with what the local memory can represent. Presenting the model with one word at a time, or separating words by zero vectors rather than an actual token, allows it to build a memory that respects the data structure. If a space character were included as an actual token, it would be treated like any other feature, leading the model to learn correlations involving it. This would break locality, and the model would no longer distinguish between word-forming and non-word-forming sequences. Space would be learned as part of words, not as a boundary, and the accepted strings of the model would no longer correspond to linguistic units. The model would simply learn a different interpretation of the data—one that reflects statistical artifacts of the tokenization, not the underlying structure of language.

This is not a deficiency, but a reflection of how learning occurs in the model. Because it has no global objective, and no access to the meaning of individual symbols, the model aligns new information with structures that have already emerged from past correlations. When trained on unstructured noise—such as a uniform string of randomly chosen letters—the model still forms memory traces. It

does so by capturing those accidental patterns in the noise that align with the allowed DAG growth. The result is a memory of accepted strings whose **collective statistical properties closely match the morphological structure of natural language**. In this sense, the model is capable of discovering natural linguistic patterns without data, because its internal memory structure **mirrors the same constraints that shape human word formation** [14]. Including a space token misleads the model, not because it fails to recognize it, but because it has no way of knowing that such a symbol is meant to indicate a boundary, rather than a letter.

Thus it provides a *scientific explanation* for the universal tokenizability of human language, not just because it processes language data in a locally coordinated (and therefore biologically plausible) way, but because it can tell us why the data exists in the first place.

8.2 Scaling Up

Scaling up the model introduces unique challenges. Naively treating the retokenizer as a conventional tokenizer—such as byte-pair encoding (BPE) [16] or other subword segmentation [55]—misses the point entirely. The retokenizer is not a preprocessing step, but a dynamic process. It functions as a compositional short-term memory system, one that stores and retrieves accepted strings by activating memory traces across the hierarchy. Discarding this hierarchical structure and collapsing all learned n -grams into a flat vocabulary would scale poorly and break the model's inductive biases. The purpose of the retokenizer is not to produce tokens for input to another model, but to generate new feature bases through replay, enabling creative learning by aligning input structure with emergent memory.

While subword segmentation methods such as byte-pair encoding (BPE) [16] and unigram language modeling [34] have become standard in NLP, they rely on statistical preprocessing over large corpora. A variety of recent approaches attempt to learn token boundaries from data, rather than relying on fixed preprocessing rules. These include segmentation-aware training using multiple subword candidates [34], latent segment models that infer tokenization jointly with downstream tasks [3], and byte-level systems that learn token patches directly from raw input [41, 52]. Probabilistic methods such as Bayesian word segmentation [19] and morphology induction algorithms like Morfessor [11] also aim to discover subword units in an unsupervised way. Yet all of these approaches depend fundamentally on the assumption that the data contains language. That is, the model must learn to tokenize from patterns already present in the input. If no such structure exists—such as when trained on noise—these models fail to recover meaningful segmentations, because there is no statistical signal to exploit.

In contrast, the framework presented here does not learn token boundaries from data but instead defines them as a side-effect of emergent memory dynamics. It does this by forming accepted sequences through local Hebbian dynamics constrained by a hierarchical DAG. Tokenization is not assumed, but emerges as a side effect of correlation alignment. No loss is minimized, no boundaries are enforced, and no tokens are treated as intrinsically meaningful (e.g. stop or space tokens). This allows the model to exhibit tokenizable structure even in the absence of language data—a capability

absent in systems trained on the assumption that language structure is already embedded in the dataset.

Going beyond the limitations of short-term memory thus requires solutions which don't ruin the emergence. Replay provides such a mechanism, as its minimal structure exploits the local dynamics to grow the model in a useful way. It suggests a framework where learned tokens are correlated in short-term memory structures, whose correlations are replayed in order to contribute yet more complex tokens into long-term memory. This problem is complicated by the lack of static architecture. This makes "scaling up" a game of assuming and exploring allowed structures, including which neurons are allowed to correlate in short-term memories, and the order and manner of replay.

Compression likely plays a critical role in scaling emergent structure. In this work, we focused on the simplest and most analytically tractable setting: binding subword patterns into word embeddings. Short-term memory need not store every n -gram, and the few-word examples we present are representative of general behavior. We apply an exact matrix product state (MPS) compression—equivalent to a tensor train decomposition—without truncating singular values, yielding fully disentangled feature maps and one embedding token per word. The resulting long-term memory functions as an attention-like, one-to-one key-value map over these discrete embeddings.

This exact decomposition demonstrates how structured embeddings can emerge from local memory dynamics. But the same MPS protocol naturally supports approximate compression by truncating small singular values, allowing generalization across statistically similar tokens. While we reserve empirical study of approximate compression for future work, its success in many-body physics [20–22, 42, 53, 60], and its growing adoption in machine learning under the name tensor train [29, 40, 61, 68], suggest that it may be essential for scaling this framework beyond the low-data regime.

8.3 Static vs Dynamic Learning

Lastly, while the incompatibility between emergent learning and modern NLP frameworks poses challenges for scaling and experimentation, it raises a more fundamental question: Are we trying to build models of cognition – capable of continual learning, intergenerational memory, and emergent language capacity – or are we refining static pattern recognizers? These are separate goals rooted in different paradigms of intelligence.

Current language models operate in a globally optimized regime: they treat learning as a statistical estimation problem, where the architecture is fixed and the learning dynamics are frozen into a high-dimensional variational ansatz. In this sense, such models are effectively *thermalized* – time plays no intrinsic role in learning.

Consider that "thinking" in static models means test-time compute – but in human learning, thinking is a dynamic learning process, where observed events are reprocessed. Though advances in reinforcement learning demonstrate how a pre-trained LLM can learn by reasoning to itself [70, 71], such zero-data learning is only possible because of the pretraining, and therefore not integral to how the model learns.

This contrasts with local event-driven learners, which require thinking for the model to grow beyond its initial locally-coordinated

limitations. Locally-learned events are little more than simple replayable memories stored in an uncoordinated way. Memory retrieval is therefore essential to continued learning, not just because it's useful to do so, but because it can do little else without further coordination.

8.4 Accident of Nature

Beyond the desire to advance technology, there is also the scientific question of human cognition. Global gradient descent presupposes (1) that a global notion of correctness exists (e.g a loss function), and (2) that neurons coordinate their updates to minimize it (via teaching signals [39]). Such global coordination is not only incompatible with the microscopic behavior of neurons, but may not be a description of *any* naturally occurring microscopic system. The assumption of global coordination violates a basic assumption of physics: that nature is an unconscious collection of accidents.

Attempts to justify LLMs as biologically plausible ignore this disconnect: a black-box model that passively reflects its data distribution cannot offer a generative theory of language, only an empirical fit to it. This makes drawing scientific conclusions impossible, thus leaving fundamental questions unanswered: Why is speech segmented into words? What enforces the universality of word-forming patterns? How does linguistic structure emerge in the first place, and what makes it stable across generations? Even at the low-level explored in this work, our framework addresses these questions.

9 CONCLUSION

We have introduced a fully local, objective-free framework for hierarchical language learning, where compositional structure emerges from unsupervised retokenization and replay. Rather than fitting to data, the model constructs an internal, interpretable hierarchy of features, enabling smooth, bounded morphological structures to arise even in the absence of training data.

This framework provides natural mechanisms for scaling up. Through smooth hierarchical composition and replay-based memory formation, the model can build long-range correlations, compress complex structures into efficient key-value memories, and recursively retokenize features across multiple scales. In principle, this enables the emergence of increasingly complex symbolic systems from simple local interactions.

However, scaling up without a global objective is not straightforward. Without loss functions to optimize, the growth of complexity depends on the evolutionary dynamics of replay, memory, and hierarchical interactions—analogueous to how structure emerges in systems like Conway's Game of Life [9, 50, 51] or Lenia [7, 8, 15, 44]. Progress toward richer, longer-range structure may require evolutionary strategies: introducing multiple interacting sub-networks, varying timescales of memory and replay, and selecting architectures that favor the extension of correlations over time.

A crucial distinction of this approach is that the model does not fit data – it interprets data. The system is fundamentally biased toward smooth, hierarchical DAG-like representations [5, 6, 59], which govern its construction of internal structure. This intrinsic bias explains its ability to extract natural language morphology from noise, and suggests a fundamentally different paradigm of

learning—one closer to human cognition, where models continually reinterpret the world rather than merely optimizing against a data distribution. This guarantees diversity in learning, where learned errors are reinterpreted in the context of intrinsic model structure, leading to language change instead of model collapse.

Ultimately, the broader goal is to build models that can develop an entire language from scratch, without preexisting data, by autonomously constructing a hierarchy of symbols, grammar, and meaning. By allowing multiple modalities of hierarchical learning—for example, connecting emergent symbol sequences with structured perceptual patterns like the finger-counting toy example—meaning can arise at the intersection of different feature sets tied together through replay and embedding. In this way, not only words but also concepts and their cross-modal relationships could emerge spontaneously, answering the question: “How did we go from a universe without language to a universe with language?”

CODE AVAILABILITY

<https://gitlab.com/ehlproj/ababot>

ACKNOWLEDGEMENTS

We thank Larry Moss, Ricky Simanjuntak, & Tony Beaver for comments/discussion.

REFERENCES

- [1] dataset. gregory carl carolina esperanza declan lourdes jonás rosa kyle jacob maricarmen tanner brian sergio ivonne christian daniel weston fidel álvaro thomas lucía carmen norberto zane esther angela anthony ronald maría damien leo efrén preston leonardo matias craig gage bobby wayne trey liam antonio maxwell ricardo elías oscar ronaldo albert fernanda jesse andrés kip joe cintia roman águeda paco elisabet mateo ryker gary grant preston félix cody selene javier victoria walker malik ford sara ian steven russell teresa clara amanda luciana isaiah dawson elena sofía jaime blake celia tucker sean hernando milagros natalia dennis jack clinton dexter elena avery axel.
- [2] Sudhanshu Agrawal, Wonseok Jeon, and Mingu Lee. 2024. AdaEDL: Early Draft Stopping for Speculative Decoding of Large Language Models via an Entropy-based Lower Bound on Token Acceptance Probability. arXiv:2410.18351 [cs.CL] <https://arxiv.org/abs/2410.18351>
- [3] Anonymous. 2024. Latent Segment Language Models. In *Submitted to ACL Rolling Review - June 2024*. <https://openreview.net/forum?id=4hlnLp0k4> under review.
- [4] Jimmy Ba, Geoffrey Hinton, Volodymyr Mnih, Joel Z. Leibo, and Catalin Ionescu. 2016. Using Fast Weights to Attend to the Recent Past. arXiv:1610.06258 [stat.ML] <https://arxiv.org/abs/1610.06258>
- [5] Anthony F Beavers. 2010. Typicality Effects and Resilience in Evolving Dynamic Associative Networks.. In *AAAI Fall Symposium: Complex Adaptive Systems*.
- [6] Anthony F. Beavers and Christopher D. Harrison. [n. d.]. *Information-Theoretic Teleodynamics in Natural and Artificial Systems*. 347–363. https://doi.org/10.1142/9789814374309_0018
- [7] Bert Wang-Chak Chan. 2019. Lenia: Biology of Artificial Life. *Complex Systems* 28, 3 (Oct. 2019), 251–286. <https://doi.org/10.25088/complexsystems.28.3.251>
- [8] Bert Wang-Chak Chan. 2020. Lenia and Expanded Universe. In *The 2020 Conference on Artificial Life (ALIFE 2020)*. MIT Press, 221–229. https://doi.org/10.1162/isal_a_00297
- [9] E. F. Codd. 1968. *Cellular Automata*. Academic Press, Inc., USA.
- [10] Brandon C. Colelough and William Regli. 2025. Neuro-Symbolic AI in 2024: A Systematic Review. (2025). arXiv:2501.05435 [cs.AI] <https://arxiv.org/abs/2501.05435>
- [11] Mathias Creutz, Krista Lagus, and Sami Virpioja. 2006. Unsupervised Morphology Induction Using Morphology. In *Finite-State Methods and Natural Language Processing*. Anssi Yli-Jyrä, Lauri Karttunen, and Juhani Karhumäki (Eds.). Springer Berlin Heidelberg, Berlin, Heidelberg, 300–301.
- [12] Artur d’Avila Garcez and Luis C. Lamb. 2020. Neurosymbolic AI: The 3rd Wave. (2020). arXiv:2012.05876 [cs.AI] <https://arxiv.org/abs/2012.05876>
- [13] Honghua Dong, Jiayuan Mao, Tian Lin, Chong Wang, Lihong Li, and Denny Zhou. 2019. Neural Logic Machines. (2019). arXiv:1904.11694 [cs.AI] <https://arxiv.org/abs/1904.11694>
- [14] P. Myles Eugenio. 2025. Hebbian learning the local structure of language. (2025). arXiv:2503.02057 [cs.CL] <https://arxiv.org/abs/2503.02057>

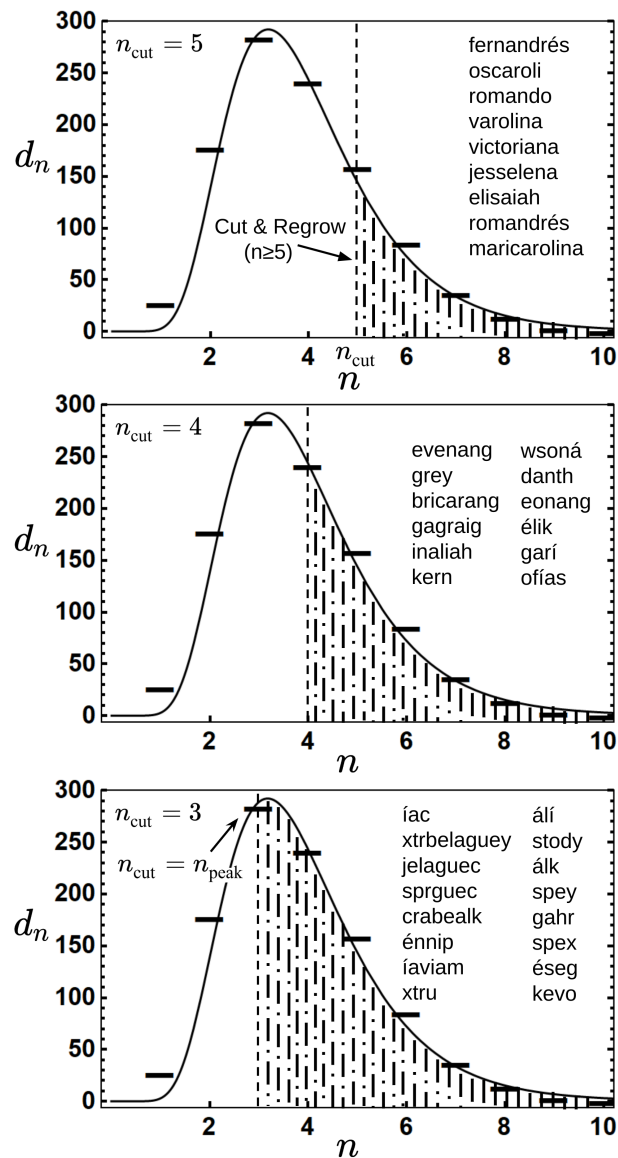


Figure 5: Number of unique n -grams in a 100-name dataset (English/Spanish mix) [1] shown as backdrop. Shaded regions mark features removed by hierarchical cuts; the solid line fits a log-normal distribution. Example words from post-cut regrowth are shown.

- [15] Maxence Faldor and Antoine Cully. 2024. Toward Artificial Open-Ended Evolution within Lenia using Quality-Diversity. arXiv:2406.04235 [cs.NE] <https://arxiv.org/abs/2406.04235>
- [16] Philip Gage. 1994. A new algorithm for data compression. *The C Users Journal archive* 12 (1994), 23–38. <https://api.semanticscholar.org/CorpusID:59804030>
- [17] Xiaocong Gan, Dahui Wang, and Zhangang Han. 2009. N-tuple Zipf Analysis and Modeling for Language, Computer Program and DNA. arXiv:0908.0500 [physics.data-an] <https://arxiv.org/abs/0908.0500>
- [18] Samuel J. Gershman, Ila Fiete, and Kazuki Irie. 2025. Key-value memory in the brain. arXiv:2501.02950 [q-bio.NC] <https://arxiv.org/abs/2501.02950>
- [19] Sharon Goldwater, Thomas L. Griffiths, and Mark Johnson. 2009. A Bayesian framework for word segmentation: Exploring the effects of context. *Cognition* 112, 1 (2009), 21–54. <https://doi.org/10.1016/j.cognition.2009.03.008>

- [20] N Gourianov. 2022. *Exploiting the structure of turbulence with tensor networks*. Ph. D. Dissertation. University of Oxford.
- [21] Nikita Gourianov, Peyman Givi, Dieter Jaksch, and Stephen B. Pope. 2025. Tensor networks enable the calculation of turbulence probability distributions. *Science Advances* 11, 5 (2025), eads5990. <https://doi.org/10.1126/sciadv.ads5990>
- [22] N. Gourianov, M. Lubasch, S. Dolgov, et al. 2022. A quantum-inspired approach to exploit turbulence structures. *Nat Comput Sci* 2, 30–37 (2022). <https://doi.org/10.1038/s43588-021-00181-1>
- [23] Alex Graves, Greg Wayne, and Ivo Danihelka. 2014. Neural Turing Machines. arXiv:1410.5401 [cs.NE] <https://arxiv.org/abs/1410.5401>
- [24] Alex Graves, Greg Wayne, Malcolm Reynolds, Tim Harley, Ivo Danihelka, Agnieszka Grabska-Barwińska, Sergio Gómez Colmenarejo, Edward Grefenstette, Tiago Ramalho, John Agapiou, Adrià Puigdomènech Badia, Karl Moritz Hermann, Yori Zwols, Georg Ostrovski, Adam Cain, Helen King, Christopher Summerfield, Phil Blunsom, Koray Kavukcuoglu, and Demis Hassabis. 2016. Hybrid computing using a neural network with dynamic external memory. *Nature* 538, 7626 (2016), 471–476. <https://doi.org/10.1038/nature20101>
- [25] Michael Hahn. 2020. Theoretical Limitations of Self-Attention in Neural Sequence Models. *Transactions of the Association for Computational Linguistics* 8 (2020), 156–171. https://doi.org/10.1162/tacl-a_00306
- [26] G. HERDAN. 1958. THE RELATION BETWEEN THE DICTIONARY DISTRIBUTION AND THE OCCURRENCE DISTRIBUTION OF WORD LENGTH AND ITS IMPORTANCE FOR THE STUDY OF QUANTITATIVE LINGUISTICS. *Biometrika* 45, 1–2 (06 1958), 222–228. <https://doi.org/10.1093/biomet/45.1-2.222> arXiv:<https://academic.oup.com/biomet/article-pdf/45/1-2/222/735477/45-1-2-222.pdf>
- [27] John E. Hopcroft, Rajeev Motwani, and Jeffrey D. Ullman. 2001. *Introduction to Automata Theory, Languages, and Computation* (2nd ed.). Addison-Wesley, Boston.
- [28] J J Hopfield. 1982. Neural networks and physical systems with emergent collective computational abilities. *Proceedings of the National Academy of Sciences* 79, 8 (1982), 2554–2558. <https://doi.org/10.1073/pnas.79.8.2554> arXiv:<https://www.pnas.org/doi/pdf/10.1073/pnas.79.8.2554>
- [29] Oleksii Hrinchuk, Valentin Khrulkov, Leyla Mirvakhabova, Elena Orlova, and Ivan Oseledets. 2020. Tensorized Embedding Layers for Efficient Model Compression. arXiv:1901.10787 [cs.CL] <https://arxiv.org/abs/1901.10787>
- [30] Jared Kaplan, Sam McCandlish, Tom Henighan, Tom B. Brown, Benjamin Chess, Rewon Child, Scott Gray, Alec Radford, Jeffrey Wu, and Dario Amodei. 2020. Scaling Laws for Neural Language Models. arXiv:2001.08361 [cs.LG] <https://arxiv.org/abs/2001.08361>
- [31] Leo Kozachkov, Ksenia V. Kastanenko, and Dmitry Krotov. 2023. Building transformers from neurons and astrocytes. *Proceedings of the National Academy of Sciences* 120, 34 (2023), e2219150120. <https://doi.org/10.1073/pnas.2219150120> arXiv:<https://www.pnas.org/doi/pdf/10.1073/pnas.2219150120>
- [32] Dmitry Krotov. 2021. Hierarchical Associative Memory. arXiv:2107.06446 [cs.NE] <https://arxiv.org/abs/2107.06446>
- [33] Dmitry Krotov and John Hopfield. 2021. Large Associative Memory Problem in Neurobiology and Machine Learning. arXiv:2008.06996 [q-bio.NC] <https://arxiv.org/abs/2008.06996>
- [34] Taku Kudo. 2018. Subword Regularization: Improving Neural Network Translation Models with Multiple Subword Candidates. In *Proceedings of the 56th Annual Meeting of the Association for Computational Linguistics (Volume 1: Long Papers)*, Iryna Gurevych and Yusuke Miyao (Eds.). Association for Computational Linguistics, Melbourne, Australia, 66–75. <https://doi.org/10.18653/v1/P18-1007>
- [35] Brenden M. Lake, Tomer D. Ullman, Joshua B. Tenenbaum, and Samuel J. Gershman. 2017. Building machines that learn and think like people. *Behavioral and Brain Sciences* 40 (2017), e253. <https://doi.org/10.1017/S0140525X16001837>
- [36] Luis C. Lamb, Artur Garcez, Marco Gori, Marcelo Prates, Pedro Avelar, and Moshe Vardi. 2021. Graph Neural Networks Meet Neural-Symbolic Computing: A Survey and Perspective. (2021). arXiv:2003.00330 [cs.AI] <https://arxiv.org/abs/2003.00330>
- [37] Xianzhi Li, Ethan Callanan, Xiaodan Zhu, Mathieu Sibue, Antony Papadimitriou, Mahmoud Mahfouz, Zhiqiang Ma, and Xiaomo Liu. 2025. Entropy-Aware Branching for Improved Mathematical Reasoning. arXiv:2503.21961 [cs.CL] <https://arxiv.org/abs/2503.21961>
- [38] Eckhard Limpert, Werner A. Stahel, and Markus Abbt. 2001. Log-normal Distributions across the Sciences: Keys and Clues: On the charms of statistics, and how mechanical models resembling gambling machines offer a link to a handy way to characterize log-normal distributions, which can provide deeper insight into variability and probability—normal or log-normal: That is the question. *BioScience* 51, 5 (05 2001), 341–352. [https://doi.org/10.1641/0006-3568\(2001\)051\[0341:LNDATS\]2.0.CO;2](https://doi.org/10.1641/0006-3568(2001)051[0341:LNDATS]2.0.CO;2) arXiv:<https://academic.oup.com/bioscience/article-pdf/51/5/341/26891292/51-5-341.pdf>
- [39] Ori Maoz, Gašper Tkačič, Mohamad Saleh Esteki, and Elad Schneidman. 2020. Learning probabilistic neural representations with randomly connected circuits. *Proceedings of the National Academy of Sciences* (2020). <https://doi.org/10.1073/pnas.191280411>
- [40] Alexander Novikov, Dmitry Podoprikhin, Anton Osokin, and Dmitry Vetrov. 2015. Tensorizing Neural Networks. arXiv:1509.06569 [cs.LG] <https://arxiv.org/abs/1509.06569>
- [41] Artidoro Pagnoni, Ram Pasunuru, Pedro Rodriguez, John Nguyen, Benjamin Muller, Margaret Li, Chunting Zhou, Lili Yu, Jason Weston, Luke Zettlemoyer, Gargi Ghosh, Mike Lewis, Ari Holtzman, and Srinivasan Iyer. 2024. Byte Latent Transformer: Patches Scale Better Than Tokens. arXiv:2412.09871 [cs.CL] <https://arxiv.org/abs/2412.09871>
- [42] Daniel E. Parker, Xiangyu Cao, and Michael P. Zaletel. 2020. Local matrix product operators: Canonical form, compression, and control theory. *Phys. Rev. B* 102 (Jul 2020), 035147. Issue 3. <https://doi.org/10.1103/PhysRevB.102.035147>
- [43] Mary Phuong and Marcus Hutter. 2022. Formal Algorithms for Transformers. arXiv:2207.09238 [cs.LG] <https://arxiv.org/abs/2207.09238>
- [44] Erwan Plantec, Gautier Hamon, Mayalen Etcheverry, Pierre-Yves Oudeyer, Clément Moulin-Frier, and Bert Wang-Chak Chan. 2023. Flow-Lenia: Towards open-ended evolution in cellular automata through mass conservation and parameter localization. arXiv:2212.07906 [cs.NE] <https://arxiv.org/abs/2212.07906>
- [45] Jorge Pérez, Pablo Barceló, and Javier Marinković. 2021. Attention is Turing-Complete. *Journal of Machine Learning Research* 22, 75 (2021), 1–35. <http://jmlr.org/papers/v22/20-302.html>
- [46] Jorge Pérez, Javier Marinković, and Pablo Barceló. 2019. On the Turing Completeness of Modern Neural Network Architectures. arXiv:1901.03429 [cs.LG] <https://arxiv.org/abs/1901.03429>
- [47] Ruizhong Qiu, Zhe Xu, Wenxuan Bao, and Hanghang Tong. 2025. Ask, and it shall be given: On the Turing completeness of prompting. In *The Thirteenth International Conference on Learning Representations*. <https://openreview.net/forum?id=AS8SPtYBw>
- [48] Hubert Ramsauer, Bernhard Schäfl, Johannes Lehner, Philipp Seidl, Michael Widrich, Thomas Adler, Lukas Gruber, Markus Holzleitner, Milena Pavlović, Geir Kjetil Sandve, Victor Greiff, David Kreil, Michael Kopp, Günter Klambauer, Johannes Brandstetter, and Sepp Hochreiter. 2021. Hopfield Networks is All You Need. arXiv:2008.02217 [cs.NE] <https://arxiv.org/abs/2008.02217>
- [49] Tobias Reinhart and Gemma De las Cuevas. 2022. The grammar of the Ising model: A new complexity hierarchy. arXiv:2208.08301 [cond-mat.stat-mech] <https://arxiv.org/abs/2208.08301>
- [50] Paul Rendell. 2011. A Universal Turing Machine in Conway’s Game of Life. In *2011 International Conference on High Performance Computing & Simulation*. 764–772. <https://doi.org/10.1109/HPCSim.2011.5999906>
- [51] Paul Rendell. 2014. *Turing Machine Universality of the Game of Life*. Ph. D. Dissertation. University of the West of England. <https://uwe-repository.worktribe.com/preview/822581/thesis.pdf>
- [52] Craig W. Schmidt, Varshini Reddy, Chris Tanner, and Yuval Pinter. 2025. Boundless Byte Pair Encoding: Breaking the Pre-tokenization Barrier. arXiv:2504.00178 [cs.CL] <https://arxiv.org/abs/2504.00178>
- [53] Ulrich Schollwöck. 2011. The density-matrix renormalization group in the age of matrix product states. *Annals of Physics* 326, 1 (2011), 96–192. <https://doi.org/10.1016/j.aop.2010.09.012> January 2011 Special Issue.
- [54] Caleb Schultz Kisby, Saúl A. Blanco, and Lawrence S. Moss. 2024. What Do Hebbian Learners Learn? Reduction Axioms for Iterated Hebbian Learning. *Proceedings of the AAAI Conference on Artificial Intelligence* 38, 13 (Mar. 2024), 14894–14901. <https://doi.org/10.1609/aaai.v38i13.29409>
- [55] Mike Schuster and Kaisuke Nakajima. 2012. Japanese and Korean voice search. In *2012 IEEE International Conference on Acoustics, Speech and Signal Processing (ICASSP)*. 5149–5152. <https://doi.org/10.1109/ICASSP.2012.6289079>
- [56] R. Shankar. 1994. Renormalization-group approach to interacting fermions. *Rev. Mod. Phys.* 66 (Jan 1994), 129–192. Issue 1. <https://doi.org/10.1103/RevModPhys.66.129>
- [57] Ramamurti Shankar. 2017. *Quantum Field Theory and Condensed Matter: An Introduction*. Cambridge University Press, Cambridge. <https://doi.org/10.1017/9781139044349>
- [58] Toby Simonds. 2025. Entropy Adaptive Decoding: Dynamic Model Switching for Efficient Inference. arXiv:2502.06833 [cs.LG] <https://arxiv.org/abs/2502.06833>
- [59] Zach Solan, David Horn, Eytan Ruppin, and Shimon Edelman. 2005. Unsupervised learning of natural languages. *Proceedings of the National Academy of Sciences* 102, 33 (2005), 11629–11634. <https://doi.org/10.1073/pnas.0409746102> arXiv:<https://www.pnas.org/doi/pdf/10.1073/pnas.0409746102>
- [60] E. Miles Stoudenmire. 2022. A Quantum-Inspired Algorithm for Solving Differential Equations. *Condensed Matter Journal Club* (2022). <https://doi.org/10.36471/JCCM-November-2022-03>
- [61] Zhan Su, Yuqin Zhou, Fengran Mo, and Jakob Grue Simonsen. 2024. Language Modeling Using Tensor Trains. arXiv:2405.04590 [cs.CL] <https://arxiv.org/abs/2405.04590>
- [62] Danil Tyulmankov, Ching Fang, Annapurna Vadaparty, and Guangyu Robert Yang. 2021. Biological learning in key-value memory networks. arXiv:2110.13976 [q-bio.NC] <https://arxiv.org/abs/2110.13976>
- [63] Ashish Vaswani, Noam Shazeer, Niki Parmar, Jakob Uszkoreit, Llion Jones, Aidan N. Gomez, Łukasz Kaiser, and Illia Polosukhin. 2017. Attention is all you need. In *Proceedings of the 31st International Conference on Neural Information*

- Processing Systems* (Long Beach, California, USA) (*NIPS'17*). Curran Associates Inc., Red Hook, NY, USA, 6000–6010.
- [64] Gail Weiss, Yoav Goldberg, and Eran Yahav. 2018. On the Practical Computational Power of Finite Precision RNNs for Language Recognition. arXiv:1805.04908 [cs.LG] <https://arxiv.org/abs/1805.04908>
 - [65] Robert L. West, Spencer Eckler, Brendan Conway-Smith, Nico Turcas, Eilene Tomkins-Flanagan, and Mary Alexandria Kelly. 2024. Bridging Generative Networks with the Common Model of Cognition. (2024). arXiv:2403.18827 [cs.AI] <https://arxiv.org/abs/2403.18827>
 - [66] C. B. WILLIAMS. 1940. A NOTE ON THE STATISTICAL ANALYSIS OF SENTENCE-LENGTH AS A CRITERION OF LITERARY STYLE. *Biometrika* 31, 3-4 (03 1940), 356–361. <https://doi.org/10.1093/biomet/31.3-4.356> arXiv:<https://academic.oup.com/biomet/article-pdf/31/3-4/356/499025/31-3-4-356.pdf>
 - [67] Kenneth G. Wilson and J. Kogut. 1974. The renormalization group and the ϵ expansion. *Physics Reports* 12, 2 (1974), 75–199. [https://doi.org/10.1016/0370-1573\(74\)90023-4](https://doi.org/10.1016/0370-1573(74)90023-4)
 - [68] Mingxue Xu, Yao Lei Xu, and Danilo P. Mandic. 2024. TensorGPT: Efficient Compression of Large Language Models based on Tensor-Train Decomposition. arXiv:2307.00526 [cs.CL] <https://arxiv.org/abs/2307.00526>
 - [69] Shimao Zhang, Yu Bao, and Shujian Huang. 2024. EDT: Improving Large Language Models' Generation by Entropy-based Dynamic Temperature Sampling. arXiv:2403.14541 [cs.CL] <https://arxiv.org/abs/2403.14541>
 - [70] Andrew Zhao, Yiran Wu, Yang Yue, Tong Wu, Quentin Xu, Yang Yue, Matthieu Lin, Shenzhi Wang, Qingyun Wu, Zilong Zheng, and Gao Huang. 2025. Absolute Zero: Reinforced Self-play Reasoning with Zero Data. arXiv:2505.03335 [cs.LG] <https://arxiv.org/abs/2505.03335>
 - [71] Xuandong Zhao, Zhewei Kang, Aosong Feng, Sergey Levine, and Dawn Song. 2025. Learning to Reason without External Rewards. arXiv:2505.19590 [cs.LG] <https://arxiv.org/abs/2505.19590>
 - [72] G. K. Zipf. 1949. *Human behavior and the principle of least effort*. Addison-Wesley Press.

10 SUPPLEMENTARY

10.1 hierarchical feature mixing via short-term memory

We stress that the role of the retokenizer is *not* to learn to tokenize data, nor store many n -grams at once. It isn't optimized to train on large data sets (nor is it necessary). When combined with replay to generate LTM tokens, all the words in a data string can be learned in chunks (even as small as one word) per STM→replay→LTM cycle. Hence the toy examples discussed in the main text are representative of how the model behaves in general.

The retokenizer is a compositional short-term memory, with the purpose of constructing new feature basis. It behaves as a correlation engine, which builds new features ($\tilde{v}^{(n)}$) from relevant local correlations ($\tilde{v}^{(n-1)}v$) when they align with a hierarchical DAG. This can occur two ways: (1) From correlations at the v -level, such as either external data (noise or structured) passed as input, or information retrieved into v from LTM. Or (2), directly sampling a uniform distribution for the elements of $g^{(n)}$ – i.e random growths.

Here we employ the cut®row method, discussed in the main text, in order to explore the hierarchical structure inspired from the features of 100 proper English or Spanish names. This minimal dataset highlights that the retokenizer, as a short-term memory mechanism, is not designed to memorize all possible n -grams of a language; and to allow the reader to inspect the generated vocabulary, to verify that the preserved $n < n_{\text{cut}}$ grams come from the initial vocabulary. The goal here is not exhaustive coverage, but to reveal how hierarchical structure emerges from feature overlaps. The limited data emphasizes that complex structure can be explored—and meaningfully represented—with remarkably little input. (And in the next section, we show how no explicit data is necessary.)

Step 1: We train a hierarchy against the 100 words, with the following hyperparameters: $\xi_g = .0001$ & $\epsilon_n = 0$ for all n . Doing this grows a hierarchy containing all the morphological features in the 100 training names.

Step 2: We choose n_{cut} and discard layers $n \geq n_{\text{cut}}$. We then randomly regrow new layers by randomly growing the $g_{\mu_{n-1},k}^{(n)}$ (same as in previous section). This grows a new vocabulary, which we extract through random replay. (We choose $N_r = 200$ replays, but more can be used to extract more words if desired.)

The produced words exhibit a mixed featureset. The n -grams of the original 100 names form the nodes of a graph defining its smooth tokenset. New tokens, generated by cutting and regrowing the hierarchy layers, preserve the original notion of smoothness up until the cut ($n_{\text{cut}} - 1$). This guarantees that new names are well-formed blends of both language morphologies.

In what follows, we show a sequence of random name regenerations for the 100 words, starting from $n_{\text{cut}} \gg n_{\text{peak}}$. Because randomly sampled $0 \leq g_{\mu_{n-1},k}^{(n)} \leq 1$, then we need choose $0 \leq \epsilon_n \leq 1$. We choose $\epsilon_{n_{\text{cut}}} > 0$ when necessary to prevent the effective dimension from blowing up beyond our computational limitations; $\epsilon_n = .5$ for a chosen $n > n_{\text{cut}}$, in order to break up long words; and else $\epsilon_n = 0$.

100 word data string: **gregory carl carolina esperanza declan lourdes jonás rosa kyle jacob maricarmen tanner brian sergio ivonne christian daniel weston fidel álvaro thomas lucía carmen norberto zane esther angela anthony ronald maría damien leo efrén preston leonardo matías craig gage bobby wayne trey liam antonio maxwell ricardo elías oscar ronaldo albert fernanda jesse andrés kip joe cintia roman águeda paco elisabet mateo ryker gary grant preston félix cody selene javier victoria walker malik ford sara ian steven russell teresa clara amanda luciana isaiah dawson elena sofía jaime blake celia tucker sean hernando milagros natalia dennis jack clinton dexter elena avery axel**

High cuts $n_{\text{cut}} \gg n_{\text{peak}}$ preserve the original morphology almost completely, thus regrowing those cuts tends to mostly reproduce the original vocabulary, and only a handful of new words.

$n_{\text{cut}} = 6$: **milagr clintonio hernanda maricardo lucian milagro**

Lowering n_{cut} reduces the constraints, allowing for more novel growths.

$n_{\text{cut}} = 5$: **jessell dexteresa amandrés oscarmen dexterestonio declara granthony presthe russelena javie westonio oscaro victoriana esperanthy celiam christiana ivonner álvarolintonio jessel espera esperantonio cintiana sergi milagrosa matia álvarolintiana granthomas pacob celisabet fernandrés maricarl presthernandrés presa granza alberto maricarolina prestherando leonaldo**

Turning on $\epsilon_n > 0$ for $n > n_{\text{cut}}$ controls word length.

$n_{\text{cut}} = 5$ & $\epsilon_7 = .5$ (to regulate word length): **fernandrés oscaroli romando agrosa lagros isabet varolina estoni vonner granto oscarm victoriana granza nthomas maliam perantoni peranza taliam omanda scarmen hernan amandré maricaroli icardo intonio exterest declara eranthony briana usselen stonio presther ricarme onardo pacob**

$n_{\text{cut}} = 5$ & $\epsilon_8 = .5$ (to regulate word length): **icarmen maliam álvarol aricarl homandré jessell estonio alberto milagrosa lisabet xteresto lvarolinto briana hernandré ivonner homando amandrés eranthomas orbeto celiam western ctoriana oscaro**

ernanda eonaldo jesselena declara presa pacob ronardo xteresa peranza lisaiah sselene

$n_{\text{cut}} = 5$ & $\epsilon_9 = .5$ (to regulate word length): **celisabet briana alberto presa milagrosa sthernando granthon cintonio ranthony ronardo celiam oscardo oscaroli elisaiah clintonio natalik peranthomas ctoriana romandrés matia arolinti aricardo western westonio leonaldo jesselena christiana álvaroli pacob thomanda presther exteresa ivonner romanda erantonio maricard sthernandrés maricarolina jesselene aricarmen nataliam restherna declara**

$n_{\text{cut}} = 5$ & $\epsilon_{10} = .5$ (to regulate word length): **maricarolina maliam briana westherna granza exterestonio alberto thernanda nthomanda victoriana celiam presa milagrosa granthomandrés lvarolina ivonner romanda maricardo declara natalik christiana leonaldo jesselena nataliam celisaiah perantoni peranthomas eranthony westonio oscardo maricarl celisabet arolintiana granthony carolinton amandrés álvarolinto romando russelena cintonio esthernandrés**

$n_{\text{cut}} = 5$ & $\epsilon_{11} = .5$ (to regulate word length): **clintiana oscardo natalik ivonner cintiana thomandrés fernandrés milagrosa hernandrés dexteresa presa granza ronardo cintonio nataliam presthernandr dexterestonio alberto romandrés rolintiana maricaroli esperanthy maricardo esperantonio álvarolinto christiana granthony russelena jesselena westonio jesselene victoriana pacob sthernando declara leonaldo speranthomas celisabet**

As $n_{\text{cut}} \rightarrow n_{\text{peak}}$, the new names begin to lose a recognizably English or Spanish structure. The longest correlations become increasingly replaced by randomness. By the time $n_{\text{cut}} = n_{\text{peak}}$, all but the most local correlations from original data are lost. Taking $n_{\text{cut}} = 2$ is equivalent to generating a random language without starting data.

$n_{\text{cut}} = 4$ & $\epsilon_4 = .7$ (to regulate exploding d_n): **kern luci noryk eonnisa inaliah honi delis exter iang evenang grey ilanert zannisa evene resto denang saranat inalis vony álvarom zanza pack élik thert sarl bricard lbery águe ianth eclarannisa forb ssern cell xeles lías ofias xwesth gelis ronnie ndaw amanth águedam riamien mari prey danth eclake álvarol rtoryk zannie pern ianert ofia sserang soni lberey iando eonang narm xwel fide rgio dang delake desaiamil malke gagraig iell xelis ctonás bricarang sserannisa resp eclaranat**

$n_{\text{cut}} = 4$ & $\epsilon_4 = .7$ (to regulate exploding d_n) & $\epsilon_5 = .5$ (to regulate word length): **ranal arme iang wsoná atía mand yleó tucí liah lene homa ictoná weleo hery perg bern zann gros onne mane cari oric saronn zang hony yner ilar essel axwe amarde tresti serg grom ianz denn gelik dest stonio omat clane joná edama feraim rony nthé sarona wald cland álvar ciandr amardo aric hris ofias maxe stoná eres xelí gela xteo mena rdell rant hric araim frén matev garí tery riam pert sabe into hera oryke stonn**

$n_{\text{cut}} = 4$ & $\epsilon_4 = .7$ (to regulate exploding d_n) & $\epsilon_6 = .5$ (to regulate word length): **wesai iant axell herey xwesth caronant bland caronat xwele heres caris teven clin homal carolin amari selin ykery onant wayn jaco isary amat rber tonn iell vict hony varai luci ylenn eanda danda honá ilake ykere agelin javi kersp jonat jaim ntord jesteo veresp gronant aliam ianio thera ierg oryk manio rdenarí jonis manz rosab nzananz nzanio ucía**

$n_{\text{cut}} = 4$ & $\epsilon_4 = .7$ (to regulate exploding d_n) & $\epsilon_7 = .5$ (to regulate word length): **walb toná ynernata thom drés selik dene ucke omaraim seliann uedang feryk preg rbernata tana uedant estord prey ronniel javi omaxe lvaronni eona inang iamalke imen thoná aynert frés avergí scar heryk gard axwes aker spernatí clianni frén heraim iamas ngell ndaws axwe aniert tianzannieli amielí lenarme bria olint mant élis mando ranieraim agranza zannisa egord jonisa cranzannieli**

$n_{\text{cut}} = 3$ & $\epsilon_3 = .9$ (to regulate exploding d_n): **íac xtrbelaguey jelaguec sprguec crabealk énnip áll áldaiabealk useg ixweny ésega sprger inzaguey ása hom iss kevo íaviv áli xtrbeax énniv ásahr spry catu orger grlv xtrt keolici spey xtru boeny ong der ixeari maw rnzaguec patu craiabealk fos íaviam dedo orguey íxeax crabelaguey rikici álk spex vedo tan deax áso íavip brm lelaguec ésealk xtrbldaiickl keoliclrv rnzarí stoeny craiam uth malk fofi élv yniv íaviob leny gahr fré jelaguey deahom stody rne lelaguey xtrbldac vayll gahom ony**

10.2 learning patterns in the noise

The following vocabulary was learned from noise:

ehqi nod lez pvp vpqn by idl khg adr uyfuq lp mfx nz zfb vhytjzf bg euq uqiq yfbp aiz eeh dxiw mv ytd qiqfl rleu aid wxiqt xgeu eht onr oqg tdzfo mnr ofod ccai vpv vhytjz drl xix eze adxge adxgehq qg fleh wof zk iqp khy mwo ud

The noise is the uniform string (shown below). We highlight those accidental correlations which trigger growths (given $\epsilon_2 = .002$, $\epsilon_{n>2} = 0$, & $\xi_g = .001$):

vncyhxkkdkfpgkwxouulfbvmbaclkhzrilyizgwygtppbbsijxehqiylpuggepponrtmlnzabnrmneeqaizbobswspemagnqkfvhjhfnfixlezdnsvfzfmnrrouuddjmbghyaxalwsbijxdeehbliqeyosamfljuhnikthjtjtqogwpgvkkcvxdpjdafekufuyoanhacaduprsbjonaouytyxgxbflehaiilavmopnaimodiqtrdrljheksenwvggjlrbgnhcdpkzkalwxcxrqi ofaerbdtj slc nr sja b p y n d c p w w i c r c x z x q b t p f i w l q d g y n i x p r c q t x c e w m d c a u d d v z t s i w l b g u q i q a e v y f l d f k q n k u y b o l x w q b z p d a i d q g m a d f k y s t m n s g x l n o w h d v p k c a f l d z u d w u v w o k e e i f d y s y i x c e h t z o q f s t j k b g j j x m s z k l h d r h m x w q y p h o m o d r z j z n z i x m g x k y a y q o p h x h z y n e u q c i p q t o s r w w k o v q w e i m e x r o e a d x g e h g k l b p d z r e v d z x q h w l b f x l p o l c y m v c f r z d w o f q t c z k s k r n o o y f r p l e m k r c c p p q f x a t d j v u g j l p k q o f m w j a l r l d b t j h s u a o j o i z n b o r x m u q s d k k x n j w x i q t e e j w y p a m v e w k h y v p u i t d z f o t k e b y g z s s c i f z k i q z q d x v t i z b y q i f l y e z l p c n z a f o z p v p u a y u x s p g g v v t c f b q s x a r o m z f b h g a e s t k j n y c a u c m q j i w h t i v p q n c e k y r l e u h q q p x v p v z e j s l r t u n e x f o n q a c m f x c c a i o q g r r h o s k w z d l q g n r b m g u d c o f o d o b i d l g i c j d x i w v b p b j z l s z e q u n j m f h t h s y v h y t j z f y w t f n t y f b p e v i r l f t p a d r i m n p c y t d h e m t q f i q p t d m v k m h y y b y m e z e n n z w e o f a q k h g i d g s o t v h p f q p v y r j n n o d a h h f u m w x h y c k d l o q n u y f u q y z o n x x g e u m w o h q i

Minimize energy by inserting spaces (i.e zero vectors). The lowest-energy tokenized state:

v n c y h x k k d k f p g k w x o u u l f b v m b a c l k h z r i l y i z g w y g t p p b b s i j x e h q i y l p u g e g p p o n r t m l n z a b n r m n e e q a i z b o b s w s p e m a g n q k f v h j h n f i x l e z d n s r i t v f z f a m n r o u u d d j m b g h y x a l w s b i j x d e e e h b l i q e y o s a m f l j u h n i k t h j t j t q o g w p g v k k c v x d p j d a f e k u f u y o a n h a c a d u p r s b j o n a o u y t y x g b x f l e h a i l a v m o p n a i k m o d i q t c r d r l j h e k x e n w v g g j l r b g n h c d p k z k a l w c x r q i o f a e r b d n t j s l c n r s j a b p y n d c p w w i c r c x z x q b t p f i w l q d g y n i x p r c q t x c e w m d c a u d d v z t s i w l b g u q i q a e v y f l d f k q n k u y b o l x w q b z p d a i d q g m a d f k y s t m n s g x l n o w h d v p k c a f l d z u d w u v w o k e e i f d y s y i x c e h t z o q f s t j k b g j j x m s z k l h d r h m x w q y p h o m o d r z j z n z i x m g x k y a y q o p h x h z y n e u q c i p q t o s r w w k o v q w e i m e x r o e a d x g e h g k l b p d z r e v d z x q h w l b f x l p o l c y m v c f r z d w o f q t c z k s k r n o o y f r p l e m k r c c p p q f x a t d j v u g j l p k q o f m w j a l r l d b t j h s u a o j o i z n b o r x m u q s d k k x n j w x i q t e e j w y p a m v e w k h y v p u i t d z f o t k e b y g z s s c i f z k i q z q d x v t i z b y q i f l y e z l p c n z a f o z p v p u a y u x s p g g v v t c f b q s x a r o m z f b h g a e s t k j n y c a u c m q j i w h t i v p q n c e k y r l e u h q q p x v p v z e j s l r t u n e x f o n q a c m f x c c a i o q g r r h o s k w z d l q g n r b m g u d c o f o d o b i d l g i c j d x i w v b p b j z l s z e q u n j m f h t h s y v h y t j z f y w t f n t y f b p e v i r l f t p a d r i m n p c y t d h e m t q f i q p t d m v k m h y y b y m e z e n n z w e o f a q k h g i d g s o t v h p f q p v y r j n n o d a h h f u m w x h y c k d l o q n u y f u q y z o n x x g e u m w o h q i

Thus we can see the hierarchical DAG structure living accidentally in the uniform string. For the hyperparameters given, bigrams are only learned if they show up at least twice in the string (because $\epsilon_2/\xi_g = 2$). The word **ehqi** is only learned because its bigrams show up at least one more time (beyond **ehqi** itself) elsewhere in the string, such as how **eh** appears in **adxgehg**, **fleh**, & **eeeh**.

Note that were we to instead have chosen $\epsilon_n = 0$ for all n , the model would attempt to learn *all* correlations in the string. The model therefore attempts to learn the entire string as a smooth tokenset, which results in it only learning a single long word.

By choosing $\epsilon_2 > 0$, we tell the model to *not* learn all observed bigrams. These now “non-word-forming” bigrams are perceived as boundaries between smooth regions of the string, thus breaking up the string into smaller words. Further turning on $\epsilon_3 > 0$ would break up the string into yet smaller words, formed from smooth trigrams & bigrams. As we subsequently fix each ϵ_n to a finite value, we’d find the words continue to break up until smaller chunks. This continues until n larger than the largest chunks ($n = n_{\max}$). At this point, the value of $\epsilon_{n > n_{\max}}$ has no effect on learning, as there are no words in the string of that length.

Different choices of the hyperparameters ϵ_n result in the string breaking up in different ways, with the strongest effect coming from learned n -grams at early n . We can therefore think of a smooth vocabulary as one possible tokenizable representation “living” inside the uniform string. Different tokenizable representations are possible given the statistics of the n -grams and the hyperparameters.

Fig’s 6 show the d_n distribution for the learned random language vocab & the noise it was learned from. Additionally, we plot d_n for the same noise string broken up by randomly inserting spaces. The hierarchical DAG structure of the random language exhibits a smooth transition across n_{peak} , in contrast to the sharp transitions exhibited by uniform chunks derived from the very same string – highlighting their distinct structural difference.

The sub-word structure of human language is the same as that demonstrated here for the random language [14], which is estimated to be a log-normal distribution [26, 38, 66]. Our model provides a bottom-up explanation for the morphological distribution of language.

10.2.1 Why is regular language structure better than context-sensitive? Because it actually teaches us something about human language & human language memory.

If the lowest-level memory system responsible for human language were context-sensitive, then it would trivially parse nested or arbitrarily embedded structures. This would allow the model to treat language as a collection of syntactically legal sequences, regardless of whether those sequences exhibit morphological coherence.

As a result, one could imagine a “language” composed of chunks of uniformly random strings, separated only by explicit delimiters (e.g a separator token or fixed syllable). A context-sensitive parser would process such input effortlessly.

However, in such a system, the distinction between word-forming and non-word-forming patterns wouldn’t be *enforced*—replaced by arbitrary token boundaries determined by structural legality rather than statistical compatibility. This lack of enforcement poses a serious

question: If the lowest level of human language memory was context-sensitive, then why hasn't a single human language evolved this (or any other similarly allowed) structure?

Therefore, in order for a singular context-sensitive system to be a valid theory of human language, some other explanation (e.g constraints) would have to be provided to account for the empirically observed universal structure. It's ability to recognize & reproduce human language data does *not* contribute to its validity as a scientific theory.

A scientific theory is one that can produce the qualities in the data without first fitting to existing data – it does not assume the data. Put another way: It must be able to learn novel language without explicit data. Our theory does that, and ties the universal structure of the data to the structural limitations of the model. This teaches us that there is a lowest level of human language (intra-word & meaning-free) which is formally regular language, and crucially, that this limitation is responsible for why human language is segmented into words.

An exhaustive exploration of language beyond this simple level is beyond the scope of this work, as it requires accounting for correlations between increasingly complex tokens. However, there is a clear motif in human language structure at all levels, such as the log-normal distributed patterns at the inter-word level [66]. This hints that the same mechanism which gives rise to the regular-language structure at the word level (the hierarchical DAG n -gram model), plays a central role at all levels of human language.

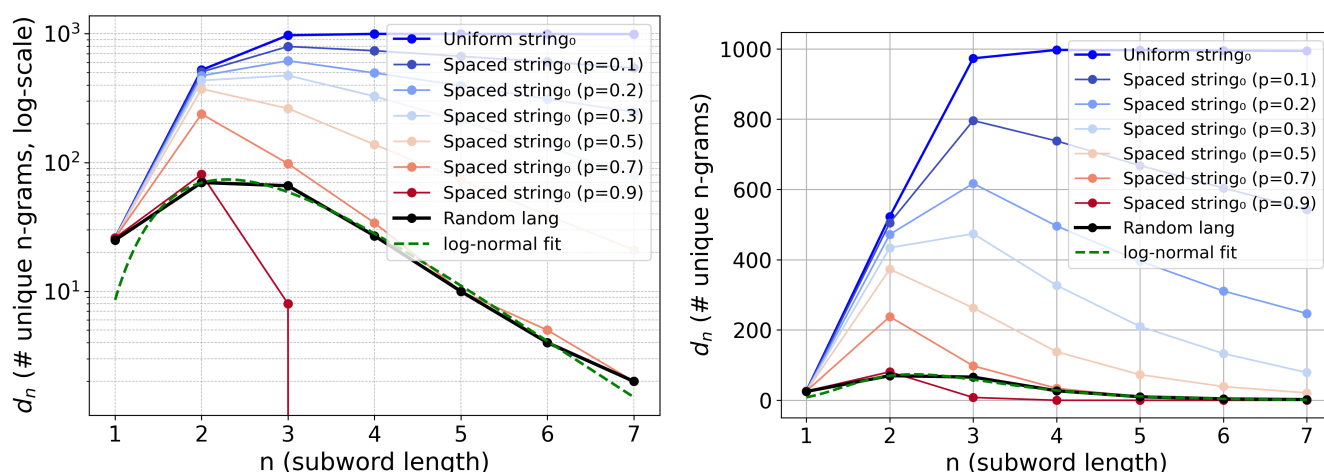


Figure 6: Emergent learning patterns in noise: Comparing d_n between the seed string₀ & the learned tokenizable representation living inside it (a.k.a random language). For comparison, seed₀ with spaces inserted at different frequencies. Even for the handful of tokenizable patterns in the string, the d_n of random language begins to approach log-normal distribution, with a smooth transition across the peak. By comparison, the transition across the peak for random strings (w/ or w/o spaces) is sharp; and its not possible to predict $d_n > d_{n_{peak}}$ from $d_n < d_{n_{peak}}$, where n_{peak} depends only on d & the sample size. Compare also Fig 7.

10.3 random synaptic growths

Growing a random language follows equivalently to Sec 10.1, except now where the entire graph is randomly learned (starting from $n = 2$). We grow this random language with the following hyperparameters: $\epsilon_n = [.9, .55, .2, .2, .3, .3]$.

`bjfyi bjfyimf cbjfa cbjfy cha chs cua cuyvea cuyveg cuyven cuyvy gpfha gpfhsl jfyi kr kv lhslhslh lyesh njfa njfac njfyia njfyim njfyin omz ow oyea oyeg oyy pfhslha plha plyea qd qnjfj qpggw qpuv rea resl rzg sfa sfhslha soql sp spf spggw tin ug vdv vdx vdxj vyesl wg xmfa xmx xw yvha yvhslh yvyi zggw zgw zmz zn`

A uniform string (noise) of equal character length to random language `bjfyi` (for comparison):

`l qvw tcprh t tsfczf uu nitxe tgsjnqb enpg mroiatiin jnjth mtteuluf fo v b tq phbk vikdvz jbhinz jkfeh nnhakwoo xnh w x hw mbs et fb xc fpg bs smnlpgx rt n g mb m k ib cxzholk granv dm oglbj rji agdfa dkew so p jwp krp w vgap qjrlzyl ggr tl o g k t n ovxrcw ctrwq o j ix ljlja e lwblvs ymkm es f e v m km j cqifdhncovhzqg fz z ygyx dx`

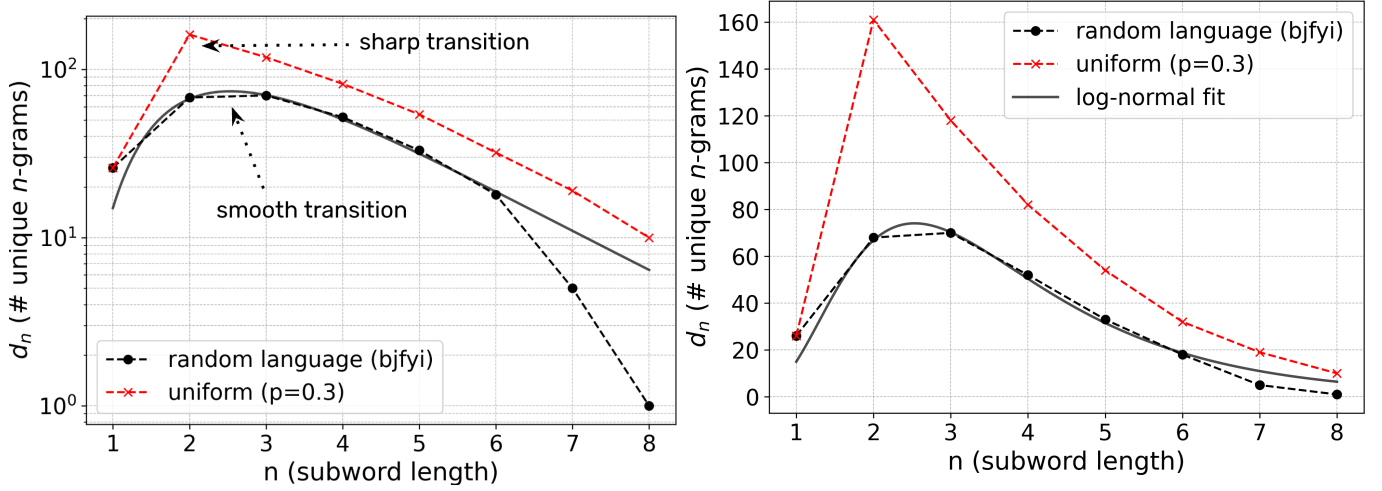


Figure 7: The distribution of word-forming patterns d_n versus pattern length n for: random language *bjfyi*, and a uniform string of equivalent number of characters (frequency $p = .3$ of inserting a space). The random language was generated by randomly growing the model layer-by-layer, with each subsequent layer constrained to be DAG-compatible with the previously grown layers (a.k.a the smoothness constraint). The d_n for a hierarchical DAG has a smooth transition, because the DAG becomes increasingly more constraining to the growth with increasing n . The peak-and-collapse is a consequence of this constraint. By contrast, for uniform strings chunks, $n < n_{\text{peak}}$ & $n > n_{\text{peak}}$ have no direct inter-relationship. The position of n_{peak} for uniform strings is set entirely by d & the string size.

10.4 Retokenizing Memory Grammars (at the word level)

We define a hierarchy of neural grammar models built on memory-encoded directed acyclic graphs (DAGs) of overlapping n -grams. The three tiers roughly correspond to languages generated by states of memory with: fixed synapses (RTG), smoothly evolving synapses via memory erasure & regrowth (CRG), and the addition of a global long-term memory (R-CRG).

10.5 Tier 1: Retokenizing Grammar (RTG)

A *Retokenizing Grammar* represents a single memory DAG encoding a word through overlapping n -grams. It is defined as:

$$\text{RTG} = (\Sigma, G)$$

where:

- Σ is a finite alphabet;
- $G = (V, E)$ is a DAG with nodes $\tau \in V \subseteq \Sigma^n$ for fixed $n \geq 2$;
- There is an edge $(\tau_1, \tau_2) \in E$ iff $\text{suffix}_{n-1}(\tau_1) = \text{prefix}_{n-1}(\tau_2)$;
- The transition $\tau_1 \wedge \tau_2 \mapsto \tau_3$ merges τ_1 and τ_2 into a new string τ_3 by overlapping the shared $(n-1)$ -gram:

$$\tau_3 = \text{merge}(\tau_1, \tau_2)$$

Each transition moves us deeper into G . A complete path through G corresponds to a sequence of such merges ending a terminating node w (the stored word). The language of an RTG is: $L(\text{RTG}) = \{w \in \Sigma^*\}$, where $\Sigma^* \subset V$. Note that nodes like **aaa** can be formed via self-mergers $\text{merge}(\mathbf{aa}, \mathbf{aa})$. A terminating node formed from self-mergers can correspond to an infinitely long word.

Token Representations and Retokenization Classes. Each string $w \in L(\text{RTG})$ corresponds to a terminating node in the DAG and defines a unique symbolic unit. However, its internal structure may admit multiple valid tokenizations via overlapping n -grams. We associate to each w a set of smooth tensor representations that describe how it may be composed from lower-order fragments.

Let $\tilde{v}_w^{(n)}$ denote the composed representation of w (an n -gram at level n), and let $\mathcal{R}(w)$ denote its retokenization class:

$$\mathcal{R}(w) \subset \mathcal{T} = \text{all valid retokenized expressions over sub-tokens}$$

For example, for $w = \mathbf{aba}$, we may have:

$$\mathcal{R}(\mathbf{aba}) = \left\{ \tilde{v}_{\mathbf{aba}}^{(3)}, \tilde{v}_{\mathbf{ab}}^{(2)} v_a, v_a \tilde{v}_{\mathbf{ba}}^{(2)}, v_a v_b v_a \right\} \quad (43)$$

Each expression describes a valid smooth composition of $\tilde{v}_{\text{aba}}^{(3)}$ based on the available overlaps. These are not distinct outputs of the grammar, but rather different structural decompositions of the same element $w \in L$.

10.6 Tier 2: Cut-and-Regrow Grammar (CRG)

A *Cut-and-Regrow Grammar* generalizes the RTG by allowing the underlying memory DAG to evolve through a process of structural erasure and local recomposition. Rather than a fixed instance of memory, a CRG defines a family of potential memory reconstructions constrained by anchor overlap rules.

We define a CRG as a transformation:

$$\text{CRG} : \text{DAG}_{\text{initial}} \rightarrow \text{DAG}_{\text{final}}$$

where:

- $\text{DAG}_{\text{initial}} = (V_{<n_c}, E_{<n_c})$ is a truncated memory graph containing only n -grams of length $n < n_c$ (the cut threshold);
- New n -grams ($n \geq n_c$) may be regrown into $\text{DAG}_{\text{final}}$ by composing overlapping $(n-1)$ -grams from $\text{DAG}_{\text{initial}}$;
- A novel n -gram τ is valid iff it is the result of a merge or self-merge from overlapping $(n-1)$ -grams already present in the graph.

Growth proceeds locally and recursively. At each step, a new DAG is created by merging compatible anchors. This process may be terminated arbitrarily or allowed to run until structural collapse (no further growth) or infinite replay (e.g through cyclic self-mergers).

We denote:

$$\begin{aligned} \mathcal{G}_{\text{cut}} &= \text{all DAGs reachable from } \text{DAG}_{\text{initial}} \text{ via valid regrowth} \\ \text{DAG}_{\text{final}} &\in \mathcal{G}_{\text{cut}} \end{aligned}$$

As in the RTG, the language $L(\text{CRG})$ consists of terminating nodes (strings) in $\text{DAG}_{\text{final}}$, and each string $w \in L$ may admit a corresponding retokenization class $\mathcal{R}(w)$ derived from its construction history.

10.7 Tier 3: Replay-Enriched Retokenizing Grammar (R-CRG)

A *Replay-Enriched Retokenizing Grammar* extends the CRG by introducing a global long-term memory of stored word structures. Let:

$$\mathcal{M}_{\text{initial}} = \{\text{DAG}_w \mid w \in \Sigma^*\}$$

be a collection of disentangled RTGs, each encoding a stored word w .

At runtime, a subset of these memory DAGs may be reloaded into the retokenizer. The result is an entangled memory structure:

$$\text{DAG}_{\text{reloaded}} = \bigcup_{w \in \mathcal{M}_{\text{load}}} \text{DAG}_w$$

This composite structure defines a new RTG with potentially mixed anchors. Applying CRG-style cut-and-regrow operations to this DAG yields a modified instance of memory: $\text{DAG}_{\text{reloaded}} \rightarrow \text{DAG}_{\text{final}}$. We define:

$$\mathcal{M}_{\text{final}} = \mathcal{M}_{\text{initial}} \cup \text{dis}(\{\text{DAG}_{\text{final}}\})$$

where $\text{dis}(\{\text{DAG}_{\text{final}}\})$ are the disentangled (via replay relearning) memory states stored in $\{\text{DAG}_{\text{final}}\}$.

The R-CRG may thus be understood as the system defined by all possible reachable global memory states. The language $L(\text{R-CRG})$ consists of terminating strings in the active memory, or equivalently, all strings recognized by (and replayable via) its key-value memory.

Algorithm 1: Hierarchical Retokenizer Training Protocol

Input: Input sequence v , basis size $d = 26$, parameters $\{\xi_g, \epsilon_n\}$
Output: Hierarchical token memory $\{\tilde{v}^{(n)}\}$ and projectors $\{P_n\}$

- 1 Initialize one-hot vectors v_k for each symbol k in alphabet;
- 2 Set context $\tilde{v}^{(1)} \leftarrow v$ (level-1 features);
- 3 **for** $n = 2$ **to** *max-depth* **do**
- 4 Initialize $g_{\mu_{n-1},k}^{(n)} \leftarrow 0$ for all μ_{n-1}, k ;
 /* Hebbian update from input events */
- 5 **foreach** *training event* $(\tilde{v}_{\mu_{n-1}}^{(n-1)}, v_k)$ **in data** **do**
- 6 $g_{\mu_{n-1},k}^{(n)} \leftarrow (1 - \xi_g)g_{\mu_{n-1},k}^{(n)} + \xi_g \cdot \tilde{v}_{\mu_{n-1}}^{(n-1)} v_k$;
- 7 **end**
 /* Apply DAG smoothness constraint */
- 8 Zero-out elements of $g^{(n)}$ violating DAG compatibility;
 /* Define merged token vectors */
- 9 **foreach** *entry* $g_{\mu_{n-1},k}^{(n)}$ **do**
- 10 **if** $g_{\mu_{n-1},k}^{(n)} > \epsilon_n$ **then**
- 11 Define new token $\tilde{v}_{\mu_n}^{(n)}$ from (μ_{n-1}, k) ;
- 12 Define projector $P_n^{\mu_n, \mu_{n-1}, k} \leftarrow 1$;
- 13 **end**
- 14 **else**
- 15 $P_n^{\mu_n, \mu_{n-1}, k} \leftarrow 0$;
- 16 **end**
- 17 **end**
- 18 Use $\tilde{v}^{(n)}$ as input to next level;
- 19 **end**
- 20 **return** $\{\tilde{v}^{(n)}\}, \{P_n\}$;

Algorithm 2: Random Growth Protocol for Hierarchical Retokenizer

Input: Alphabet size $d = 26$, depth N , thresholds $\{\epsilon_n\}$
Output: Hierarchical memory $\{g^{(n)}\}$ and token projectors $\{P_n\}$

- 1 Initialize level-1 basis v_k : one-hot vectors for each symbol k ;
- 2 Set $\tilde{v}^{(1)} \leftarrow v$;
- 3 **for** $n = 2$ **to** N **do**
 - 4 /* Randomly initialize correlation matrix */
 - 5 Sample $g_{\mu_{n-1},k}^{(n)} \sim \mathcal{U}[0,1]$ i.i.d.;
 - 6 /* Apply DAG mask to enforce smoothness constraint */
 - 7 Zero-out elements of $g^{(n)}$ violating hierarchical DAG constraints;
 - 8 /* Construct merged token vectors */
 - 9 **foreach** (μ_{n-1}, k) **do**
 - 10 **if** $g_{\mu_{n-1},k}^{(n)} > \epsilon_n$ **then**
 - 11 Define new token $\tilde{v}_{\mu_n}^{(n)}$ from (μ_{n-1}, k) ;
 - 12 Set projector $P_n^{\mu_n, \mu_{n-1}, k} \leftarrow 1$;
 - 13 **end**
 - 14 **else**
 - 15 $P_n^{\mu_n, \mu_{n-1}, k} \leftarrow 0$;
 - 16 **end**
 - 17 **end**
 - 18 Use $\tilde{v}^{(n)}$ to define basis for next level;
- 19 **end**
- 20 **return** $\{g^{(n)}\}, \{\tilde{v}^{(n)}\}, \{P_n\}$;
